

## Extinction within the Limit of Validity of the Darwin Transfer Equations.

### I. General Formalisms for Primary and Secondary Extinction and Their Application to Spherical Crystals

BY PIERRE J. BECKER\* AND PHILIP COPPENS

*Chemistry Department, State University of New York at Buffalo, Acheson Hall, Buffalo, New York 14214, U.S.A.*

(Received 22 March 1973; accepted 10 August 1973)

A theory of extinction is derived which is valid within the limit of the Darwin intensity transfer equations. An expression describing the effect of  $n$ -fold rescattering within an ideal crystallite is derived, which differs from the equation given by Zachariasen because independent coordinates  $x_1$  and  $x_2$  based on an external coordinate system have been used, rather than the coordinates  $t_1$  and  $t_2$  which are only mutually independent if the crystal is a parallelepiped with faces parallel to the incident and diffracted beams. Furthermore, the derivation of the earlier expressions is based on a generally unjustifiable reversal of the direction of the diffracted ray (interchange of  $t_2$  and  $t_2'$ ). An exact expression is derived for the diffraction cross section  $\sigma(\epsilon_1)$  in the perfect crystallite, which contains a factor  $\sin 2\theta$  neglected in the earlier work. As a result, the previously used classification of crystals into type I and type II becomes less well defined because at very small Bragg angles particle size always becomes the dominant effect. It is shown that the extinction factor  $y_p$  ( $p$ =primary), for a perfect spherical crystallite, calculated with the present theory, is in good agreement with calculations based on the dynamical theory. Furthermore, the limiting behavior of the expressions at  $2\theta=0$  and  $\pi$  justifies some of the mathematical approximations made. For a mosaic crystal the extinction coefficient  $y$  is written as  $y_p \cdot y_s$  ( $s$ =secondary).  $y_p$  is evaluated numerically from the expressions derived. An analytical expression for  $y_p$  is obtained by least-squares fit to the numerical values. A similar procedure is followed for  $y_s$ , in the case of a Gaussian, Lorentzian and Fresnellian distributions of the crystallites and a spherical mosaic crystal. Analysis of the results shows that the Zachariasen expression can be used for small extinction ( $y > 0.8$ ), provided the  $\theta$  dependent factor is properly introduced for particle-size-affected extinction. Allowance for polarization effects in the X-ray case is discussed. Absorption effects cannot be treated separately from extinction for all but small values of  $1 - y$ . Coefficients of the analytical extinction expressions are given for absorbing spherical crystals with  $\mu R$  values  $\leq 4$ . Application of the expressions and extension to non-spherical geometries will be treated in following publications.

#### Introduction

The theory of extinction in X-ray diffraction (Zachariasen, 1967) – here referred to as  $Z$  – has been applied to a variety of cases (Zachariasen, 1968*a*, *b*, *c*, 1969). In general, significant improvements were achieved in comparison to the results of earlier treatments (Zachariasen, 1963; James, 1957). The theory has been generalized to include anisotropic extinction effects and expressions have been derived for inclusion of extinction parameters in a least-squares refinement (Coppens & Hamilton, 1970; Coppens, 1969; Larson, 1969). The theory has also been extended to include the Borrmann effect (Zachariasen, 1968*d*) in case of high absorption. Various authors have pointed out shortcomings of the theory, which are of two different natures. The most important limitation is due to the theory being of kinematical nature (Werner, 1969). It has only been applied for secondary extinction, and is limited by the approximations inherent in the mosaic model (Azaroff, 1964). Lawrence (1972) has

shown recently, using a large crystal of LiF, that the method is not very suited to correct for severe primary extinction.

It has been pointed out (Cooper & Rouse, 1970, 1971; Cooper, 1970) that it is possible to give improved solutions to Zachariasen's differential equations. Very recently (Sequeira, Rajagopal & Chidambaram, 1972*a*, *b*), an empirical improvement to the extinction correction formula has been applied in a refinement of the severely extinguished neutron intensities of L-glutamic acid. HCl. These authors also point out the existence of a correlation between conventional and extinction parameters.

Zachariasen's correction underestimates extinction and some bias can result in the thermal parameters. Especially for electron-density analysis, it is necessary to have unbiased thermal parameters from neutron diffraction. Ideally, the extinction treatment should be based on the dynamical theory (Takagi, 1961; Authier, 1970). As no general solutions using this theory are known, we decided to reconsider carefully the Darwin transfer equations used by Zachariasen, comparing whenever possible the results with those from dynamical calculations. In the course of this

\* Permanent address: Centre de Mécanique Ondulatoire Appliqué, 23 rue du Maroc, 75019 Paris, France.

analysis, some quite fundamental errors in Zachariasen's solution became apparent. As a result, the modifications by Cooper & Rouse also have to be reconsidered. Using a different procedure, we have obtained an improved formalism for both primary and secondary extinction, suitable for inclusion in a refinement program, and applicable to spherical or ellipsoidal crystals (Becker & Coppens, 1974). The present article will consist of three parts. After a general treatment of the problem, the formalism will be applied to spherical crystals. Subsequently, polarization and absorption effects are considered. In following articles examples of application of the new theory will be studied and the theory will be generalized to a crystal of more general shape and to anisotropic extinction.

Most of the mathematical derivations can be found in the first four Appendices of this article.

## I. General formalism

### I. 1. Review of the kinematical theory

Let us first review some important results of the kinematical theory of diffraction by an ideal crystal [see for example Azaroff (1968)]. It is assumed that all the observations are made in a horizontal plane, the crystal being able to rotate about a vertical axis. Let  $\mathbf{u}_0$  and  $\mathbf{u}$  be the unit vectors along the incident and diffracted beams, which coincide with  $\mathbf{u}_0^0$  and  $\mathbf{u}^0$  when the Bragg condition is exactly fulfilled (Fig. 1).  $\boldsymbol{\tau}_1$  and  $\boldsymbol{\tau}_2$  are unit vectors in the diffraction plane, respectively perpendicular to  $\mathbf{u}_0^0$  and  $\mathbf{u}^0$ , and  $\boldsymbol{\tau}_3$  is a unit vector along the vertical axis. The diffraction vector  $\mathbf{S}$  will be defined by:

$$\begin{aligned} \mathbf{S} &= \mathbf{H} + \lambda^{-1}(\varepsilon_1 \boldsymbol{\tau}_1 + \varepsilon_2 \boldsymbol{\tau}_2 + \varepsilon_3 \boldsymbol{\tau}_3) \\ &= \mathbf{H} + \lambda^{-1} \boldsymbol{\varepsilon} \end{aligned} \quad (1)$$

where  $\mathbf{H}$  is the reciprocal vector corresponding to a given reflection. The intensity of radiation scattered in direction  $\mathbf{u}$  is given by:

$$I_k(\boldsymbol{\varepsilon}) = \mathcal{J}_0 \left| \frac{aFK}{R_0} \right|^2 \left| \sum_{\mathbf{L}} \exp(2\pi i \lambda^{-1} \boldsymbol{\varepsilon} \cdot \mathbf{L}) \right|^2 \quad (\text{Z. 22})$$

where the symbols are defined in the glossary (Appendix E). The power recorded in the counter,  $P_k(\varepsilon_1)$ , which depends only on the small divergence  $\varepsilon_1$  of the incident beam from  $\mathbf{u}_0^0$  is given by:

$$P_k(\varepsilon_1) = R_0^2 \iint I_k(\boldsymbol{\varepsilon}) d\varepsilon_2 d\varepsilon_3. \quad (\text{Z. 23})$$

The diffracting cross section per unit volume and unit intensity is defined by:

$$\sigma(\varepsilon_1) = \mathcal{J}_0^{-1} v^{-1} P_k(\varepsilon_1). \quad (4) \quad (\text{Z. 20})$$

$\sigma(\varepsilon_1)$  is assumed to be constant inside the crystal, and dependent only on the size and shape of the average mosaic domain. Finally, the quantity  $Q$ , average cross

section per unit volume of crystal, is obtained by integration of  $\sigma(\varepsilon_1)$  over  $\varepsilon_1$

$$\begin{aligned} Q &= v^{-1} |aFK|^2 \iiint \left| \sum_{\mathbf{L}} \exp(2\pi i \lambda^{-1} \boldsymbol{\varepsilon} \cdot \mathbf{L}) \right|^2 d\varepsilon_1 d\varepsilon_2 d\varepsilon_3 \\ &= (\lambda^3 / \sin 2\theta) \cdot |aFK|^2 v^{-1} \sum_{\mathbf{L}} \sum_{\mathbf{L}'} \delta(\mathbf{L} - \mathbf{L}')^* \end{aligned}$$

which gives the known result:

$$Q = \left| \frac{aFK}{V} \right|^2 \lambda^3 / \sin 2\theta. \quad (5)$$

The kinematical integrated intensity  $\mathcal{P}_k$  is:

$$\mathcal{P}_k = \int P_k(\varepsilon_1) d\varepsilon_1 = \mathcal{J}_0 v Q. \quad (6)$$

If extinction effects are now introduced, the integrated intensity becomes  $\mathcal{P}$ , which is related to  $\mathcal{P}_k$  by:

$$\mathcal{P} = \mathcal{P}_k \cdot y \quad (7)$$

where  $y$  is the extinction factor which has to be calculated.

### I. 2. Extinction in an ideal crystal

Given a crystal of known shape, it is possible using previous arguments, to calculate  $\sigma(\varepsilon_1)$ . One of the major assumptions in what follows is that, when allowing for mutual coupling between incident and diffracted beams, the diffracting unit cross section remains  $\sigma(\varepsilon_1)$  at any point inside the crystal. If one considers a section of the crystal in a plane parallel to the diffraction plane (Fig. 2), a coordinate system is defined with an origin  $O$  and axes parallel to the incident and to the diffracted directions (coordinates  $x_1$  and  $x_2$ ). The coordinate  $x_3$  is taken along the vertical axis. As the angles  $\varepsilon_i$  which allow for measurable diffracted intensity are very small, the variations of  $\mathbf{u}_0$  and  $\mathbf{u}$  from  $\mathbf{u}_0^0$  and  $\mathbf{u}^0$  can be neglected in geometrical calculations. For a point  $M$  inside the crystal, with

\*  $\delta(\mathbf{u} - \mathbf{a})$  represents a Dirac distribution centered at point  $\mathbf{a}$ .

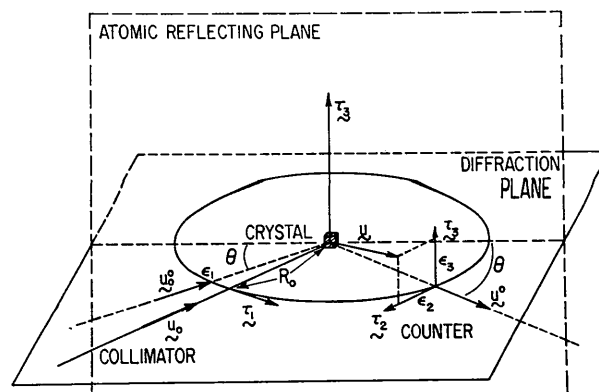


Fig. 1. Definition of the directions of the incident beam  $\mathbf{u}_0$  and of the diffracted beam  $\mathbf{u}$  with respect to their ideal values  $\mathbf{u}_0^0$  and  $\mathbf{u}^0$  (defining the diffraction plane), when the Bragg condition is fulfilled.  $R_0$  is the distance between the crystal and the counter.

coordinates  $x_1$  and  $x_2$ , the points  $M_1^0, M_1^1, M_2^0, M_2^1$  are those defined on Fig. 2, with respective coordinates  $(x_1^0, x_2), (x_1^1, x_2), (x_1, x_2^0), (x_1, x_2^1)$ . It is important to notice that  $x_1^0$  and  $x_1^1$  are functions of  $x_2$  (given by the equation of the limiting surface of the crystal) and that  $x_2^0$  and  $x_2^1$  are functions of  $x_1$ . The following distances are defined:

$$\begin{aligned} t_1 &= \overline{M_1^0 M} = x_1 - x_1^0 \\ t_2 &= \overline{M_2^0 M} = x_2 - x_2^0 \\ t_2' &= \overline{M M_2^1} = x_2^1 - x_2, \end{aligned} \quad (8)$$

where  $t_1$  and  $t_2'$  are the path lengths pertinent for absorption factor calculations. The intensity of the scattered beam at point  $M$  will be  $I(M)$ , that of the incident beam being  $I_0(M)$ . These intensities are subject to the boundary conditions:

$$\begin{aligned} I_0(M_1^0) &= \mathcal{I}_0 \\ I(M_2^0) &= 0. \end{aligned} \quad (9)$$

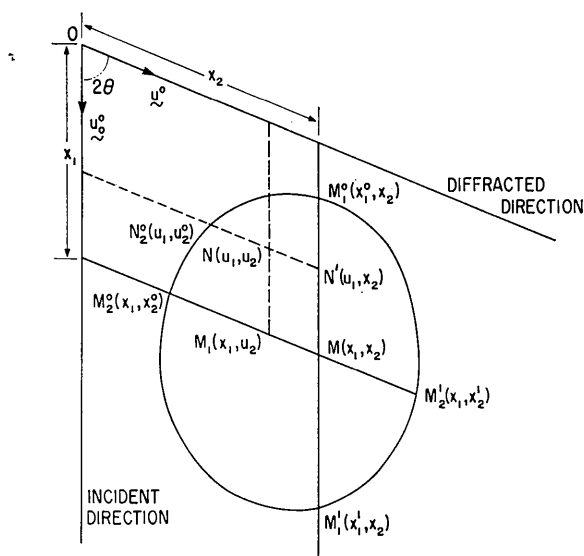


Fig. 2. Section of the crystal in a plane parallel to  $\mathbf{u}_0^0$  and  $\mathbf{u}^0$ , the incident and diffracted directions. The coordinates of each point of interest are written in parentheses.  $t_1 = \overline{M_1^0 M}$ ;  $t_2' = \overline{M M_2^1}$ .

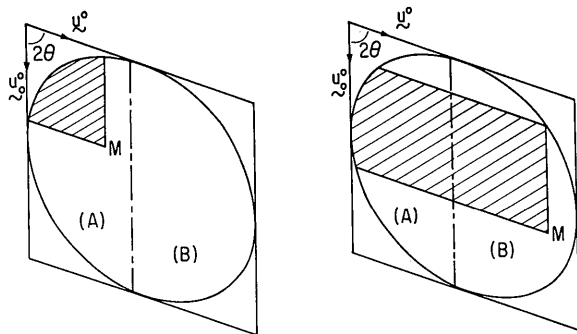


Fig. 3. The two geometrical situations for a point  $M$  in the crystal, for the integration of equation (11). The area to be considered in (11) is the shaded one.

If the exchange of energy between incident and diffracted beams at various points is considered (Zachariassen, 1965), one gets:

$$\frac{\partial I_0}{\partial x_1} = -\sigma(I_0 - I) \quad (10a)$$

$$\frac{\partial I}{\partial x_2} = -\sigma(I - I_0) \quad (10b)$$

$$\frac{\partial I_0}{\partial x_1} + \frac{\partial I}{\partial x_2} = 0. \quad (10c)$$

These equations differ from those of Zachariassen, in which  $t_1$  and  $t_2$  are considered independent variables, instead of  $x_1$  and  $x_2$ . As a result, Zachariassen's solutions and those of Cooper & Rouse (1970) are only correct for the particular case of a parallelepiped whose edges are parallel to  $\mathbf{u}_0^0$  and  $\mathbf{u}^0$ , so that  $x_1$  and  $x_2$  are equal to  $t_1$  and  $t_2$ , and for an infinite parallel plate, where there is a linear relationship between  $t_1$  and  $t_2$ .

It is shown in Appendix A how the intensity  $I_0$  at point  $M(x_1, x_2)$  is related to  $I_0$  at the preceding points  $N(u_1, u_2)$  such that radiation travels from  $N$  to  $M$  by a single rescattering (Fig. 2). With the variables defined in Fig. 2, the result can be written:

$$\begin{aligned} I_0(x_1, x_2) &= \mathcal{I}_0 \exp(-\sigma t_1) + \sigma^2 \{ \exp[-\sigma(x_1 + x_2)] \\ &\times \int_{x_1^0}^{x_1} du_1 \int_{u_2^0}^{x_2} I_0(u_1, u_2) \exp[\sigma(u_1 + u_2)] du_2 \} \end{aligned} \quad (11)$$

[relation (A3)]. The power of the diffracted beam,  $P(\varepsilon_1)$  is given by (A2)

$$P(\varepsilon_1) = \sigma \int_v I_0(x_1, x_2) \exp(-\sigma t_2') dv. \quad (12)$$

Then the function  $\varphi(\sigma)$  is defined by the relation:

$$P(\varepsilon_1) = \mathcal{I}_0 v \sigma \varphi(\sigma) = P_k(\varepsilon_1) \varphi(\sigma) \quad (13) \text{ (Z. 7)}$$

so that from (7) one gets:

$$y = Q^{-1} \int \sigma \varphi(\sigma) d\varepsilon_1 \quad (14) \text{ (Z. 9)}$$

where, from (12) and (13),  $\varphi(\sigma)$  can be written as:

$$\varphi(\sigma) = v^{-1} \mathcal{I}_0^{-1} \int_v dv I_0(M) \exp(-\sigma t_2'). \quad (15)$$

When  $\varphi(\sigma)$  and  $\sigma(\varepsilon_1)$  are known, (14) allows derivation of the extinction factor  $y$  for an ideal crystallite.

*Calculation of  $\varphi(\sigma)$ :*  $\varphi(\sigma)$  is calculated by iterative use of the relation (11), where the area being considered in the integration is the shaded area shown in Fig. 3, for the two geometrically distinct situations (provided that the limiting surface of the crystal is convex). Applying (11)  $k$  iterative times allows for  $2k$ -fold exchange of the intensity between the incident and the diffracted beams before point  $M$  is reached. Each iteration adds a term in which the power in  $\sigma$  is increased by 2 and

accordingly a power series in  $\sigma$  can be obtained (Appendix B) where the term with power  $(2p)$  in  $\sigma$  corresponds to the  $2p$ -fold rescattering contribution. For example, the first-order approximation ( $k=0$ ) which neglects the feedback term  $\sigma I$  in equation (10a) gives the solution:

$$I_0 = \mathcal{J}_0 \exp(-\sigma t_1) \quad (16a)$$

$$\varphi(\sigma) = v^{-1} \int_v dv \exp[-\sigma(t_1 + t'_2)] \quad (16b)$$

according to (15). It is the expected result,  $\sigma$  acting as an apparent absorption coefficient. The solution (Z. 11) given by Zachariassen (1967) involves  $t_2$  instead of  $t'_2$ , and as a result it applies to an angle  $(\mathbf{u}_0, \mathbf{u})$  equal to  $(\pi - 2\theta)$  (inversion of the diffracted beam into  $-\mathbf{u}$ ), rather than to the intended angle  $2\theta$ .

As discussed in Appendix B, the general solution, allowing for multiple scattering, can be approximated by:

$$\varphi(\sigma) \simeq v^{-1} \int_v dv \exp[-\sigma(t_1 + t'_2)] \mathcal{J}_0[2i\sigma v / (t_1 t'_2)] \quad (17)$$

where  $\mathcal{J}_0(x)$  is a zero-order Bessel function.

It is also shown in Appendix B that the result for  $\varphi(\sigma)$  can be expressed in terms of a power series in  $\sigma$ :

$$\begin{aligned} \varphi(\sigma) = 1 - \sigma t^{(1)} + \frac{\sigma^2}{2!} t^{(2)} + \dots \\ + (-1)^n \frac{\sigma^n}{n!} t^{(n)} + \dots \end{aligned} \quad (18a)$$

with

$$t^{(n)} = \sum_{j=0}^n \binom{n}{j}^2 v^{-1} \int_v dv t_1^j t_2^{n-j}. \quad (18b)$$

It appears that (18) is the same series as the solution (Z. 14) given by Zachariassen for a parallelepiped with two edges parallel to  $\mathbf{u}_0^0$  and  $\mathbf{u}^0$ , provided we replace  $t_2$  by  $t'_2$  [interchange of angles  $(2\theta)$  and  $(\pi - 2\theta)$ ]. Because of the symmetry with respect to  $(2\theta = \pi/2)$  in this particular case, the resulting values for  $\varphi(\sigma)$  are the same.

The approximations necessary to derive (17) for a crystal of arbitrary convex shape indicate that this formula is very appropriate for low Bragg angles (where the extinction effect is the most severe). For high Bragg angles  $\varphi(\sigma)$  defined by (17) is somewhat overestimated, which implies an underestimate of the extinction. For the two limit cases  $(2\theta=0)$  and  $(2\theta=\pi)$ , an exact solution can be found to equations (10) [equations (B8) and (B10) of Appendix B]. It is also shown in Appendix B that (17) gives the exact limit for  $2\theta=0$ . For  $2\theta=\pi$  it will be shown below, for a spherical crystal, that the error made using (18) is only of the third power in  $\sigma$ . As the extinction is very small for  $2\theta=\pi$ , we can conclude that (17) and (18) are a reasonable approximation for crystals of general shape in the whole range of Bragg angles.

The solutions given by Cooper & Rouse (1970)

partially correct the wrong variation with  $\theta$  of Zachariassen's theory. Their correction assumes that (Z. 14) is valid for  $(2\theta=0)$ ; as a result the expression is not valid for very small or very large angles of diffraction, though it gives a reasonable fit for angles of medium value.

It may be mentioned that the solution given by Zachariassen for an infinite parallel plate (Z. 12–Z. 13) is valid, because of the symmetry in  $t_2$  and  $t'_2$  for this particular geometry.

*Calculation of  $\sigma(\varepsilon_1)$ :* For a crystal with a convex limiting surface it is possible to evaluate exactly the diffracting cross section  $\sigma(\varepsilon_1)$  (Appendix C), as defined by equations (2)–(4). The result is:

$$\sigma(\varepsilon_1) = Qv^{-1} \int_v dv \cdot \alpha \cdot \frac{\sin^2 \pi \varepsilon_1 \alpha}{(\pi \varepsilon_1 \alpha)^2} \quad (19a)$$

where

$$\alpha = l \sin 2\theta / \lambda \quad (19b)$$

if  $l$  is the thickness of the crystal, parallel to the diffracted beam. The expression (19) is different from the formulas used in previous treatments (Zachariassen, 1967; Cooper & Rouse, 1970), where:

$$\begin{aligned} \sigma(\varepsilon_1) \sim Q\alpha_0 \frac{\sin^2 \pi \varepsilon_1 \alpha_0}{(\pi \varepsilon_1 \alpha_0)^2} \quad (20) \quad (Z. 24) \\ \alpha_0 = \bar{t}_\perp / \lambda \end{aligned}$$

where for spherical crystals  $\bar{t}_\perp$  was interpreted as the average thickness, in a direction parallel to the diffraction plane  $(\mathbf{u}_0^0, \mathbf{u}^0)$  and perpendicular to  $\mathbf{u}_0^0$  (mean thickness parallel to  $\tau_1$ ). The main difference is the occurrence of an additional factor  $\sin 2\theta$ ; it is clear that the definition of  $t_\perp$  must be incorrect, because it would give an infinite value for  $\sigma(\varepsilon_1)$  at  $2\theta=0$  in the case of an infinite plane parallel plate.

It will be shown below that  $\sigma(\varepsilon_1)$  can be calculated exactly using (19) for various shapes of crystals.

### I. 3. Extinction in a mosaic crystal

The mathematical treatment is similar in the case of a mosaic crystal. Equations (10) remain of the same form but  $x_1$  and  $x_2$  are now variables which span the mosaic crystal, with the same boundary conditions as before. If the misorientation of the various crystallites is considered, the incident beam striking a given crystallite makes an angle  $(\varepsilon_1 + \eta)$  with the ideal Bragg direction if  $\varepsilon_1$  is still the external divergence angle of the incident beam and  $\eta$  is the misalignment angle of the crystallite. As a result, the diffracting cross section inside this crystallite is  $\sigma(\varepsilon_1 + \eta)$ . It is possible to define an angular distribution  $W(\eta)$  for the crystallites. If one considers the travel of the incident and diffracted beams inside the mosaic crystal, outside a given crystallite,  $\sigma(\varepsilon_1)$  in equation (10) is replaced by:

$$\begin{aligned} \bar{\sigma}(\varepsilon_1) &= \int \sigma(\varepsilon_1 + \eta) W(\eta) d\eta \\ \bar{\sigma}(\varepsilon_1) &= \sigma * W \end{aligned} \quad (21)$$

if it is assumed that all crystallites are of the same average shape.

This function  $\bar{\sigma}(\varepsilon_1)$ , which is the mean diffracting unit cross section inside the mosaic crystal, corresponds to the secondary extinction effect. Because they describe transfer of intensity, the equations (10) are physically more realistic for evaluating secondary extinction than for primary extinction (Werner, 1969), since scattering becomes incoherent when randomly oriented domains are considered. Expression (21) describes two broadening effects of the reflection curve: the particle size effect in  $\sigma$ , giving a half width  $\varepsilon_\sigma$  which is inversely proportional to the effective particle size  $\langle l \sin 2\theta \rangle$ , and the mosaic-spread distribution, described by a half width  $\varepsilon_w$ . There are two important limiting cases:

(1) The effective particle size is the dominant effect determining the width of the reflection curve. Thus, when  $\langle l \sin 2\theta \rangle$  is small (in which case primary extinction is negligible:

$$\bar{\sigma}(\varepsilon_1) \sim \sigma(\varepsilon_1). \quad (22)$$

This corresponds to the type II crystal defined by Zachariasen ( $\varepsilon_\sigma \gg \varepsilon_w$ ). It should be noted that, because of the  $\sin 2\theta$  dependence, for any particle size, any crystal will behave as type II crystals for very small Bragg angles.

(2) If on the contrary, the particle size is large or the mosaic spread is small ( $\varepsilon_\sigma \ll \varepsilon_w$ ) the secondary extinction is dominated by the mosaic distribution (type I crystal) and thus:

$$\bar{\sigma}(\varepsilon_1) \sim QW(\varepsilon_1). \quad (23)$$

In this case, it becomes necessary to consider the travel of the beams within a perfect crystallite. For a given incident beam direction (a given  $\varepsilon_1$ ), primary and secondary extinction effects may, in first approximation, be considered as independent, or

$$\varphi(\varepsilon, W) \simeq \varphi_p(\sigma) \cdot \varphi_s(\bar{\sigma})$$

(the indices  $p$  and  $s$  refer to primary and secondary extinction). The same assumption will be used in averaging over various values of  $\varepsilon_1$ , which leads to:

$$y \simeq y_p \cdot y_s. \quad (24)$$

A similar assumption has been used by various authors (Hamilton, 1957, 1963; Chandrasekhar, 1956). As  $\varphi_p(\sigma)$  is generally not very different from 1, the approximation (24) is believed to be reasonable. This is confirmed by the application of (24) to neutron intensity data on  $\text{SrF}_2$  and to  $\text{LiF}$  (Becker & Coppens, 1973).

## II. Detailed solution of the transfer equations for specific crystal shapes, especially spheres

### II. 1. Perfect infinite parallel plate

An analytical solution can be found to equations (10), which coincides with the solution given by Zachariasen (1967). In the symmetrical Laue case:

$$\varphi(\sigma) = \{1 - \exp(-2\sigma\bar{t})\}/2\sigma\bar{t} \quad (25a) \quad (\text{Z. 12})$$

where  $\bar{t} = D_0/\cos \theta$  ( $D_0$ : thickness of the plate).  $\bar{t}$ , the mean path length through the crystal, coincides with the thickness  $l$  of the crystal, parallel to the direction of diffraction [see equation (19)].

In the symmetrical Bragg case,  $\varphi(\sigma)$  is given by

$$\varphi(\sigma) = 1/(1 + \sigma\bar{t}) \quad (25b) \quad (\text{Z. 13})$$

with

$$\bar{t} = l = D_0/\sin \theta.$$

The present theory gives for  $\sigma(\varepsilon_1)$  the solution (19)

$$\sigma(\varepsilon_1) = Q\alpha \frac{\sin^2(\pi\varepsilon_1\alpha)}{(\pi\varepsilon_1\alpha)^2}$$

with

$$\alpha = l \sin 2\theta/\lambda$$

or, for the two symmetrical cases,

$$\begin{aligned} \alpha_{\text{Laue}} &= 2D_0 \sin \theta/\lambda \\ \alpha_{\text{Bragg}} &= 2D_0 \cos \theta/\lambda. \end{aligned}$$

In comparison, the values for  $\alpha$  in the expression derived by Zachariasen for  $\sigma(\varepsilon_1)$  [equation (20)] are too small by a factor of two.

If  $\varphi(\sigma)$  is expanded in a power series, one gets for both Bragg and Laue cases:

$$\varphi(\sigma) \sim 1 - \sigma\bar{t} + \dots$$

and the primary extinction correction  $y_p$  (14) is given by:

$$y_p \sim Q^{-1} \int \sigma d\varepsilon_1 - Q^{-1}\bar{t} \int \sigma^2 d\varepsilon_1 + \dots$$

Thus:

$$y_p \text{ (present theory)} \sim 1 - \frac{2}{3}Q\alpha\bar{t} + \dots \quad (27a)$$

The dynamical theory has been extensively discussed for an infinite parallel plate (Zachariasen, 1945; James, 1963). The series expansion for primary extinction is given by:

$$y_p \text{ (dynamical theory)} \sim 1 - \frac{1}{3}Q\alpha\bar{t} + \dots \quad (27b)$$

The agreement with dynamical theory obtained by Zachariasen for the parallel plate is unfortunately due to errors in his derivation of  $\sigma(\varepsilon_1)$ ; it must be concluded that the transfer equations (10) incorrectly describe the primary extinction effect in an infinite parallel plate.

### II. 2. Perfect spherical crystal

The dynamical theory, in a first-order approximation, gives for primary extinction in a sphere of radius  $r$  (Weiss, 1952; Ekstein, 1951):

$$y_p \text{ (dynamical theory)} = 1 - \frac{7}{4}(Qr^2 \sin 2\theta/\lambda) + \dots \quad (28)$$

The function  $\sigma(\varepsilon_1)$  can be derived exactly (Appendix D) for a sphere:

$$\sigma(\varepsilon_1) = \frac{3}{4}Q\beta \frac{(\pi\varepsilon_1\beta)^2 - (\pi\varepsilon_1\beta) \sin(2\pi\varepsilon_1\beta) + \sin^2(\pi\varepsilon_1\beta)}{(\pi\varepsilon_1\beta)^4} \quad (29)$$

where

$$\beta = 2r \sin 2\theta/\lambda.$$

If  $\varphi(\sigma)$  is taken as the series expansion (18), integrating  $\sigma\varphi(\sigma)$  over the angle  $\varepsilon_1$  gives\*

$$y_p \text{ (present theory)} = 1 - \frac{9\sigma}{70}(Qr^2 \sin 2\theta/\lambda) + \dots \quad (30)$$

Thus the present theory agrees reasonably well with the dynamical results for a spherical crystal.

*Calculation of  $\varphi(\sigma)$  for  $2\theta=0$  or  $2\theta=\pi$ :* A closed form for  $\varphi(\sigma)$  can only be obtained for the two cases ( $2\theta=0$ ) and ( $2\theta=\pi$ ). Using equations (B8) and (B9) of Appendix B, it can be shown that:†

$$\varphi^0(\sigma r) = \frac{3}{64(\sigma r)^3} \{8(\sigma r)^2 + 4\sigma r \exp(-4\sigma r) - [1 - \exp(-4\sigma r)]\} \quad (31)$$

$$\varphi^\pi(\sigma r) = \frac{3}{4(\sigma r)^3} \{(\sigma r)^2 - (\sigma r)^{\frac{1}{2}} + \ln(1 + 2\sigma r)\}. \quad (32)$$

As noted previously, the limit of the solution given by either equation (17) or equation (18) is not exact, for  $2\theta=\pi$ .

It is interesting to compare the two results for  $2\theta=\pi$ . As  $(\sigma r)$  is always small for high diffraction angles, a series expansion of (32) is possible and gives:

$$\varphi^\pi(\sigma r) = 1 - \sigma r + \frac{1}{15}(\sigma r)^2 - \frac{9}{80}(\sigma r)^3 + \frac{2}{5}(\sigma r)^4 + \dots \quad (33a)$$

where  $\bar{t}$  is the mean thickness of the crystallite ( $\frac{3}{2}r$  for a spherical crystal, Appendix D). The series approximation (18) gives for  $2\theta=\pi$  (see Appendix D for the calculation of  $\bar{t}^{(n)}$ )

$$\varphi(\sigma r) \sim 1 - \sigma \bar{t} + \frac{1}{15}(\sigma \bar{t})^2 - \frac{9}{80}(\sigma \bar{t})^3 + \frac{2}{5}(\sigma \bar{t})^4 + \dots \quad (33b)$$

It can be concluded that the solution given by (17) or (18) is a second-order approximation of the exact solution for very large scattering angles. For  $\theta=0$ , (17) and (31) represent the same function, which suggests validity of (17) and (18) in the whole range of  $2\theta$  angles.

*Evaluation of  $\varphi(\sigma)$  at intermediate values of  $2\theta$ .*  $\varphi(\sigma)$  for different values of  $\theta$  and  $(\sigma r)$  has been obtained using numerical Gaussian integration of (17) (six grid points in each direction proved to give a sufficient accuracy). The results for  $[1/\varphi(\sigma r)]$  are plotted in Fig. 4. The angular dependence appears to be very important and the actual  $\varphi(\sigma r)$  differs significantly from the approximation given by Zachariasen

$$\varphi(\sigma) \sim 1/(1 + \sigma \bar{t}) \quad (Z. 19)$$

at all but small values of  $\sigma r$ .

\* From equation (29) it is possible to show that  $\int \sigma^2 d\varepsilon_1 = 33/70 Q^2 \beta$ .

†  $\varphi(\sigma)$  depends on the product  $\sigma r$  as easily seen from equations (17) and (18), and may therefore be designated as  $\varphi(\sigma r)$ .

It appears from Fig. 4 that for high values of  $(\sigma r)$ ,  $1/\varphi(\sigma r)$  tends to become linear with  $(\sigma r)$  which corresponds to total reflection (Zachariasen, 1967). Analytical fits to the results of Fig. 4 can be found, but it seems more appropriate to fit  $y$  analytically rather than  $\varphi(\sigma r)$ , as it is the quantity of ultimate interest.

The angular dependence of  $\varphi(\sigma)$  can also be evaluated from the series expansion (18), following arguments used by Cooper & Rouse (1970). The quantities  $\bar{t}^{(n)}$  were numerically calculated for various angles  $\theta$  and the following fit was tried:

$$\bar{t}^{(n)}(\theta) = \bar{t}^{(n)}(0) + \{\bar{t}^{(n)}(\pi) - \bar{t}^{(n)}(0)\} f_n(\theta). \ddagger$$

As series (18) can be slowly convergent, this analysis was done for values of  $n$  up to 16 and a reasonable fit appeared to be:

$$f_n(\theta) = \sin^{n+3/2}\theta$$

thus  $\varphi(\sigma r)$  can be written:

$$\varphi(\sigma r) \sim \varphi^0(\sigma r) + \sin^{3/2}\theta \{\varphi^\pi(\sigma r/\sin\theta) - \varphi^0(\sigma r/\sin\theta)\}. \quad (34)$$

Unfortunately, an analytical integration of  $\{\sigma\varphi(\sigma)\}$  over  $\varepsilon_1$ , using (34), is generally impossible. However, as described below an adequate formula for  $y$  can be obtained by numerical integration followed by least-squares fit to an analytical expression.

*Evaluation of the correction for primary extinction,  $y_p$ .* If  $\sigma(\varepsilon_1)$  is written as

$$\sigma(\varepsilon_1) = \sigma(0)f(\eta)$$

$$\ddagger f_n(0) = 0, f_n(\pi) = 1.$$

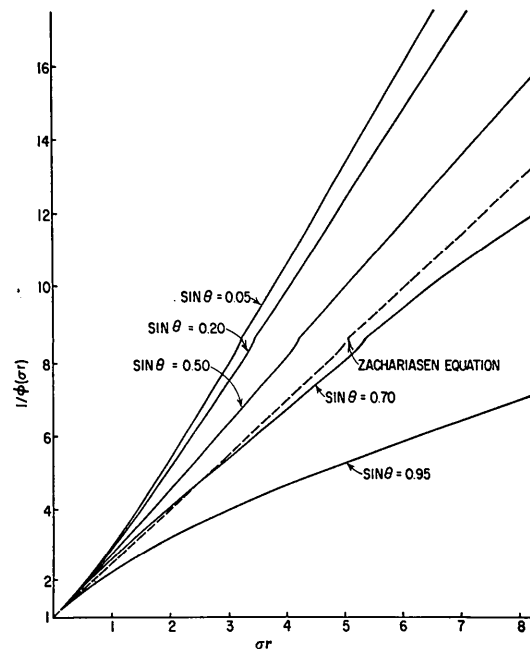


Fig. 4. Plot of  $\{1/\varphi(\sigma r)\}$  as a function of  $\{\sigma r\}$  for various  $\theta$ .

where

$$\sigma(0) = \frac{3}{4} Q\beta$$

and

$$\eta = \pi \varepsilon_1 \beta$$

$$\beta = \frac{4}{3} \bar{r} \sin 2\theta / \lambda = 2r \sin 2\theta / \lambda,$$

the quantity  $\sigma r$  becomes:

$$\sigma r = x f(\eta)$$

where

$$x = \sigma(0)r = \frac{3}{4} Q\beta r = Q\bar{\alpha}r = \frac{2}{3} Q\bar{\alpha}\bar{r} \quad (35a)$$

and  $\bar{\alpha}$  is the mean value of the parameter  $\alpha$  defined previously [equation (19)]

$$\bar{\alpha} = \frac{3}{4} \beta = \frac{3}{2} r \sin 2\theta / \lambda. \quad (35b)$$

From (14),  $y_p$  is thus given by:

$$y_p = \frac{3}{4\pi} \int_{-\infty}^{+\infty} f(\eta) \varphi[xf(\eta)] d\eta. \quad (36)$$

$y_p$  is thus only dependent on  $x$  and  $\theta$ . For given values of  $x$  and  $\theta$ , a Gaussian grid is introduced for the variable  $\eta$  and for each corresponding value of  $\{xf(\eta)\}$ ,  $\varphi(\sigma r)$  is calculated as described previously. The result of the calculation of  $y_p$  is given in Table 1 as a function of  $x$  and  $\sin \theta$ . A graphical representation is shown in Fig. 5.

An analytical expression was found by least-squares fit, in the range ( $0 < x < 30$ ), using:

$$y_p = \left\{ 1 + 2x + \frac{A(\theta)x^2}{1 + B(\theta)x} \right\}^{-1/2} \quad (37)$$

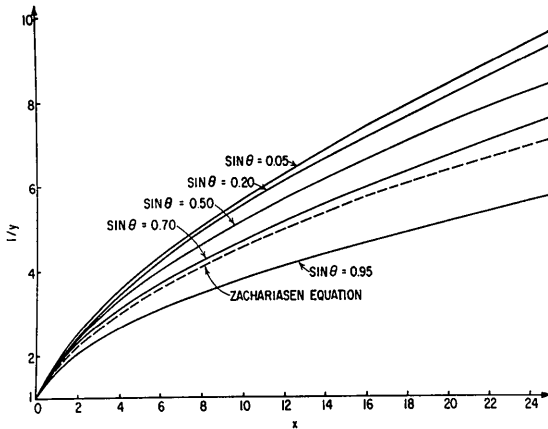


Fig. 5. Plot of the inverse of the primary extinction correction ( $1/y_p$ ) as a function of the parameter  $x$ , for various  $\theta$ .

Table 1. Primary extinction correction for a sphere, as a function of  $x = \frac{2}{3} Q\bar{\alpha}\bar{r}$  and  $\sin \theta$

	Values are multiplied by $10^4$ .									
$\sin \theta$	0.05	0.10	0.20	0.30	0.40	0.50	0.60	0.70	0.80	0.90
$x$										
0.1	9088	9091	9096	9096	9096	9096	9095	9095	9100	9107
0.2	8367	8373	8382	8382	8384	8388	8391	8399	8417	8440
0.4	7222	7231	7249	7252	7264	7280	7299	7329	7378	7438
0.6	6365	6375	6399	6410	6432	6461	6497	6549	6628	6723
0.8	5706	5716	5746	5763	5794	5835	5887	5957	6061	6185
1	5185	5198	5232	5253	5292	5343	5407	5492	5615	5763
1.5	4273	4286	4328	4360	4410	4476	4561	4670	4824	5012
2	3683	3696	3743	3780	3836	3910	4004	4125	4295	4506
2.5	3269	3282	3332	3372	3430	3508	3605	3731	3910	4134
3	2952	2975	3025	3067	3126	3204	3303	3431	3614	3846
4	2532	2544	2695	2638	2695	2772	2869	2997	3180	3418
5	2242	2253	2303	2345	2399	2474	2567	2693	2873	3111
6	2030	2040	2089	2130	2182	2253	2342	2464	2640	2875
7	1867	1876	1924	1964	2013	2081	2166	2284	2454	2685
8	1736	1744	1791	1830	1877	1941	2023	2137	2303	2529
9	1627	1636	1681	1719	1764	1825	1904	2015	2176	2397
10	1536	1544	1588	1625	1668	1727	1803	1910	2067	2283
12	1388	1396	1437	1473	1513	1568	1637	1740	1889	2095
14	1273	1280	1319	1354	1391	1443	1510	1606	1748	1946
16	1180	1186	1224	1257	1293	1342	1405	1497	1634	1824
18	1103	1108	1145	1177	1211	1257	1318	1406	1538	1722
20	1037	1042	1075	1109	1141	1185	1243	1329	1456	1634
25	0908	0913	0945	0975	1005	1045	1097	1176	1294	1460
30	0814	0820	0848	0876	0904	0940	0989	1063	1173	1330

Table 2. Variation with  $\theta$  of the least-squares-fitted coefficients  $A(\theta)$  and  $B(\theta)$  for a perfect sphere, when the primary extinction correction is  $y_p = \{1 + 2x + A(\theta)x^2 / 1 + B(\theta)x\}^{-1/2}$   
 $q(\theta)$  is the reliability factor of the fit for a given angle.

$\sin \theta$	0.05	0.10	0.20	0.30	0.40	0.50	0.60	0.70	0.80	0.90
$A(\theta)$	0.65	0.64	0.61	0.58	0.52	0.42	0.31	0.20	0.06	0
$B(\theta)$	0.18	0.18	0.19	0.21	0.21	0.20	0.19	0.18	0.13	~
$q(\theta)$	0.018	0.018	0.018	0.017	0.017	0.017	0.016	0.015	0.012	~

and varying  $A(\theta)$  and  $B(\theta)$ . The agreement factor for each value of  $\theta$  is defined as:

$$q(\theta) = \frac{\sum_{x_i} |Ay(\theta, x_i)|}{\sum_{x_i} |y|}$$

The results of this calculation are shown in Table 2. An analytical fit can be found for the  $\theta$  dependence of  $A(\theta)$  and  $B(\theta)$ :

$$\begin{aligned} A(\theta) &= 0.20 + 0.45 \cos 2\theta \\ B(\theta) &= 0.22 - 0.12 (0.5 - \cos 2\theta)^2. \end{aligned} \quad (38)$$

It is apparent from Fig. 5 that the approximation of Zachariassen can be used only for very small extinction, provided that his value for  $x$  in

$$y_p(\text{Zachariassen}) = (1 + 2x)^{-1/2} \quad (\text{Z. 27})$$

is replaced by (35a) containing the factor  $\sin 2\theta$ .

The limiting value of  $y$  for large values of  $x$  will now be compared with the results which can be expected from perfect-crystal theory (James, 1957). The limit of  $y(x)$  for large values of  $x$  according to (37) is  $(c/\sqrt{x})$ . As  $x$  is proportional to  $|F^2|$ , the integrated intensity has limit values proportional to  $|F|$ , a result in accordance with dynamical theory (James, 1957).

For the case of X-ray diffraction, the ratio  $(\mathcal{P}_\perp/\mathcal{P}_\parallel)$  of the integrated intensities relative to the perpendicular and parallel components of the electric field is known to be equal to  $|\cos 2\theta|$  for a perfect crystal (James, 1957). The present theory as expressed by (37) gives the right limit for large values of  $x$ , since  $x$  is proportional to the polarization term  $K^2$  ( $= \cos^2 2\theta$  or 1).

From these considerations and the agreement between expressions (28) and (30), it may be concluded that the present theory gives a reasonable representation of the primary extinction effect in a spherical crystal.

### II. 3. Extinction in a spherical crystal containing idealized spherical domains

The calculation of the secondary extinction correction  $y_s$  can be performed using an equation similar to (36), where  $\sigma$  is replaced by the convoluted value  $\bar{\sigma}$  [defined in (21)], and the radius of the crystal becomes  $R$ . Usually the assumption is made that the angular

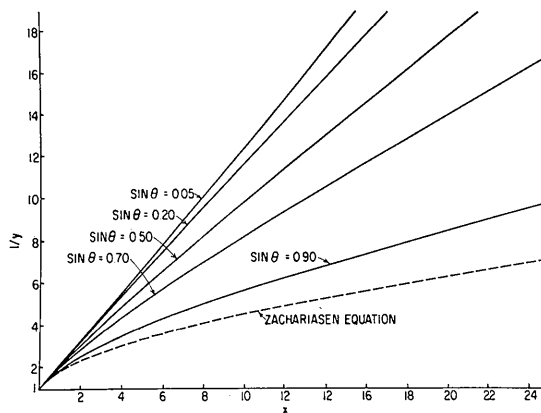


Fig. 6. Plot of the inverse of the secondary extinction correction ( $1/y_s$ ) as a function of the parameter  $X$ , for various  $\theta$ : Gaussian distribution.

Table 3. Secondary extinction correction for a sphere, as a function of  $X = \frac{2}{3} Q \alpha_G \bar{T}$  and  $\sin \theta$ , assuming a Gaussian distribution

All values are multiplied by  $10^4$ .

$x$	$\sin \theta$	0.05	0.10	0.20	0.30	0.40	0.50	0.60	0.70	0.80	0.90
0.1		9042	9045	9049	9049	9049	9049	9049	9049	9053	9063
0.2		8230	8236	8247	8247	8249	8253	8257	8267	8287	8312
0.4		6943	6953	6972	6972	6990	7008	7030	7064	7119	7187
0.6		5981	5992	6019	6031	6056	6989	6130	6189	6278	6385
0.8		5242	5254	5287	5306	5341	5387	5446	5526	5643	5783
1		4660	4673	4712	4737	4779	4837	4911	5006	5146	5312
1.5		3647	3658	3706	3742	3798	3874	3970	4094	4268	4481
2		2995	3009	3062	3104	3167	3252	3358	3495	3689	3927
2.5		2545	2559	2615	2660	2725	2815	2925	3069	3271	3524
3		2215	2229	2286	2333	2400	2489	2602	2747	2954	3215
4		1765	1777	1835	1883	1948	2036	2145	2290	2496	2763
5		1476	1482	1538	1585	1647	1731	1836	1976	2178	2445
6		1261	1272	1326	1373	1431	1510	1610	1746	1941	2204
7		1104	1114	1167	1212	1267	1342	1437	1568	1757	2013
8		0982	0991	1042	1085	1137	1209	1300	1426	1608	1858
9		0883	0892	0941	0984	1033	1100	1187	1309	1486	1729
10		0802	0810	0857	0899	0946	1011	1094	1211	1382	1619
12		0676	0682	0727	0766	0809	0869	0946	1056	1217	1442
14		0582	0587	0630	0667	0707	0762	0834	0938	1090	1304
16		0508	0514	0554	0590	0627	0679	0745	0844	0989	1193
18		0450	0455	0493	0528	0563	0612	0675	0768	0907	1102
20		0403	0407	0443	0477	0511	0556	0616	0705	0838	1026
25		0315	0319	0352	0383	0413	0453	0506	0586	0706	0878
30		0256	0259	0289	0318	0345	0381	0429	0502	0612	0772



orientations of the crystallite follow either a Gaussian with distribution:

$$W_G(\varepsilon_1) = \sqrt{2g} \exp(-2\pi g^2 \varepsilon_1^2) \quad (39a)$$

or a Lorentzian distribution:

$$W_L(\varepsilon_1) = 2g/(1 + 4\pi^2 \varepsilon_1^2 g^2). \quad (39b)$$

It is shown in Appendix D that the expression for  $\bar{\sigma}$  is much simplified if the diffracting power  $\sigma(\varepsilon_1)$  of a perfect crystallite is approximated respectively by a Gaussian or a Lorentzian distribution (D6).  $\bar{\sigma}$  is then given by one of the two following expressions:

$$\bar{\sigma}_G(\varepsilon_1) = Q\alpha_G \exp(-\pi\varepsilon_1^2\alpha_G^2) \quad (40a)$$

$$\alpha_G = \bar{\alpha} / \left(1 + \frac{\bar{\alpha}^2}{2g^2}\right)^{1/2}; \quad (40b)$$

$$\bar{\sigma}_L(\varepsilon_1) = \frac{4}{3}Q\alpha_L / \left\{1 + \left(\frac{4\pi}{3}\alpha_L\varepsilon_1\right)^2\right\} \quad (41a)$$

with

$$\alpha_L = \bar{\alpha} / \left(1 + \frac{2\bar{\alpha}}{3g}\right), \quad (41b)$$

where  $\bar{\alpha}$  is defined in equation (35b).

If  $\beta_{G,L}$  is defined by

$$\beta_{G,L} = \frac{4}{3}\alpha_{G,L}$$

and  $\eta$  is defined as previously by:

$$\eta = \pi\varepsilon_1\beta_{G,L}.$$

(36) can be applied to evaluate  $y_s$ . The parameter  $x$  [equation (35a)] is replaced by:

$$X = \frac{2}{3}Q\alpha_{G,L}\bar{T} \quad (42)$$

where  $\bar{T}$  is the mean path length through the crystal ( $= \frac{2}{3}R$  for a sphere). The results of the integrations are represented on Fig. 6 and Fig. 7 and are listed in Tables 3 and 4.

For a given extinction correction  $y_s$ , the corresponding value of  $X$  for a Lorentzian distribution is larger than for a Gaussian distribution and as a result indicates that  $\alpha_G < \alpha_L$ . This is related to the more rapid decrease of a Gaussian distribution with increasing  $\varepsilon_1$ , compared with a Lorentzian one. It is also evident that the extinction correction  $y_s$ , for a given  $Q$ , becomes closer to 1 where the Bragg angle  $\theta$  increases.

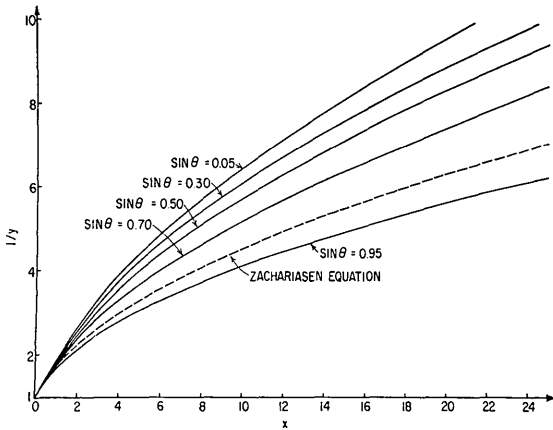


Fig. 7. Plot of the inverse of the secondary extinction correction ( $1/y_s$ ) as a function of the parameter  $X$ , for various  $\theta$ : Lorentzian distribution.

Table 4. Secondary extinction correction for a sphere, as a function of  $X = \frac{2}{3}\alpha_L Q \bar{T}$  and  $\sin \theta$ , assuming a Lorentzian distribution

All values are multiplied by  $10^4$ .

$\sin \theta$	0.05	0.10	0.20	0.30	0.40	0.50	0.60	0.70	0.80	0.90
$x$										
0.1	9005	9008	9014	9013	9013	9013	9013	9015	9021	9030
0.2	8281	8286	8296	8296	8300	8305	8310	8321	8341	8367
0.4	7174	7182	7199	7205	7218	7237	7259	7292	7365	7409
0.6	6373	6382	6496	6418	6441	6473	6511	6565	6646	6743
0.8	5769	5779	5809	5826	5857	5899	5950	6021	6123	6246
1	5297	5308	5342	5364	5400	5450	5512	5594	5713	5855
1.5	4469	4480	4521	4550	4596	4658	4735	4836	4979	5155
2	3925	3936	3980	4014	4064	4131	4215	4325	4481	4676
2.5	3534	3546	3591	3628	3679	3749	3835	3950	4113	4319
3	3237	3248	3295	3332	3384	3454	3542	3659	3825	4038
4	2809	2819	2867	2904	2956	3025	3112	3229	3397	3616
5	2510	2519	2566	2604	2654	2721	2806	2921	3088	3307
6	2285	2295	2340	2378	2426	2491	2573	2628	2850	3068
7	2108	2117	2162	2199	2245	2309	2309	2499	2659	2875
8	1947	1973	2017	2054	2098	2159	2237	2345	2502	2715
9	1845	1853	1895	1932	1975	2034	2110	2215	2370	2578
10	1742	1750	1792	1828	1870	1927	2001	2104	2255	2460
12	1577	1584	1624	1659	1699	1753	1823	1922	2068	2266
14	1446	1453	1492	1525	1564	1616	1683	1778	1918	2110
16	1341	1347	1385	1418	1454	1504	1568	1660	1796	1982
18	1253	1259	1296	1328	1363	1410	1472	1561	1692	1875
20	1179	1185	1219	1250	1285	1330	1390	1476	1604	1782
25	1033	1038	1071	1100	1132	1173	1228	1309	1428	1597
30	0925	0929	0960	0988	1018	1057	1108	1184	1296	1457

Thus the approximation of Zachariasen (Z. 27) is only valid for small values of  $X$ . An expression of the same form as equation (37) gives a satisfactory approximation to the numerical values.\* The least-squares-fitted values for  $A(\theta)$  and  $B(\theta)$  are given in Tables 5 and 6. A reasonable representation of the  $\theta$  dependence is:

$$\begin{aligned} A_G &= 0.58 + 0.48 \cos 2\theta + 0.24 \cos^2 2\theta \\ B_G &= 0.02 - 0.025 \cos 2\theta \end{aligned} \quad (43)$$

for a Gaussian distribution, and:

$$\begin{aligned} A_L &= 0.025 + 0.285 \cos 2\theta \\ B_L &= 0.15 - 0.2 (0.75 - \cos 2\theta)^2 \text{ if } \cos 2\theta > 0 \\ B_L &= -0.45 \cos 2\theta \text{ if } \cos 2\theta < 0 \end{aligned} \quad (43a)$$

for a Lorentzian distribution.

The previous treatments (Zachariasen, 1967; Cooper & Rouse, 1970) make use of the approximate function:

$$\bar{\sigma}_F(\varepsilon_1) = Q\alpha_G \frac{\sin^2(\pi\varepsilon_1\alpha_G)}{(\pi\varepsilon_1\alpha_G)^2} \quad (44)$$

which we shall call a Fresnel distribution. (Such a function takes values between those of a Lorentzian and a Gaussian distribution when the angle  $\varepsilon_1$  becomes large). The same calculations as for a Gaussian and a Lorentzian distributions have been done using  $\sigma_F(\varepsilon_1)$ . The least-squares-fitted values for  $A_F(\theta)$  and  $B_F(\theta)$  can be represented by:

$$\begin{aligned} A_F(\theta) &= 0.48 + 0.6 \cos 2\theta \\ B_F(\theta) &= 0.20 - 0.06 (0.2 - \cos 2\theta)^2, \end{aligned} \quad (44a)$$

the agreement factor  $\varrho(\theta)$  being approximately 0.02.

Finally, if  $\bar{\alpha} \gg g$  (type I crystal):

$$\bar{\alpha}_G \sim \sqrt{2}g, \quad \alpha_L \sim \frac{3}{2}g.$$

If  $\bar{\alpha} \ll g$  (type II crystal):

$$\alpha_G \sim \alpha_L \sim \bar{\alpha}.$$

\* The expression for  $y_s$  is slightly modified in the case of a Gaussian distribution:  $y_s = \{1 + 2.12X + A(\theta)X^2 / (1 + B(\theta)X)\}^{-1/2}$ , due to the fact that  $\int \sigma^2 d\varepsilon_1 = Q^2\alpha_G/\sqrt{2}$  instead of  $Q^2\alpha_L \cdot \frac{3}{2}$ .

According to the earlier theory type I and type II are the limiting cases for the scattering behavior of real crystals. The present theory predicts that the crystal type may vary with Bragg angle. Even if  $(r/\lambda \gg g)$ ,  $\bar{\alpha}$  becomes smaller than  $g$  where the Bragg angle is very small: as a result, for small-angle scattering, any crystal behaves as a type II crystal, the extinction being dominated by the particle size.

It can also be expected that  $(r/\lambda \gg g)$  when extinction is severe, since otherwise  $\alpha_{G,L}$  would be unreasonably small for small Bragg angles. Thus, for severe extinction, it can be necessary to introduce a primary extinction correction, as previously described.

### III. Polarization and absorption effects

#### III. 1. Polarization in X-ray diffraction

The quantities  $Q$  and  $x$  (or  $X$ ) are effectively reduced by polarization effects, such that

$$\begin{aligned} Q &= Q_0 K^2 \\ x &= x_0 K^2, \end{aligned}$$

where  $Q_0$  and  $x_0$  correspond to the perpendicular (unattenuated) component of the electric field (the expression for  $K$  is given in Appendix E). The two components of the integrated intensity are then:

$$\mathcal{P}_{\parallel} = \mathcal{I}_0 v Q_0 \cos^2 2\theta y_{\parallel} \quad (45a)$$

$$\mathcal{P}_{\perp} = \mathcal{I}_0 v Q_0 y_{\perp}, \quad (45b)$$

where

$$y_{\parallel} = y(x_0 \cos^2 2\theta), \quad y_{\perp} = y(x_0). \quad (45c)$$

If the X-ray incident beam is unpolarized, the average integrated intensity  $\mathcal{P}$  is:

$$\mathcal{P} = \mathcal{I}_0 v Q_0 (y_{\perp} + y_{\parallel} \cos^2 2\theta) / 2.$$

If the quantity  $p_n$  is defined as:

$$p_n = \frac{1}{2}(1 + \cos^{2n} 2\theta)$$

Table 5. Variation with  $\theta$  of the coefficients  $A(\theta)$  and  $B(\theta)$  for a mosaic spherical crystal, assuming a Gaussian distribution

$\varrho(\theta)$  is the reliability index of the least-squares fit to numerical results.

$\sin \theta$	0.05	0.10	0.20	0.30	0.40	0.50	0.60	0.70	0.80	0.90
$A$	1.30	1.28	1.19	1.11	1.00	0.88	0.74	0.60	0.44	0.26
$B$	-0.007	-0.007	-0.002	0.002	0.005	0.008	0.012	0.020	0.030	0.040
$\varrho$	0.020	0.021	0.019	0.021	0.023	0.027	0.028	0.028	0.027	0.023

Table 6. Variation with  $\theta$  of the coefficient  $A(\theta)$  and  $B(\theta)$  for a mosaic spherical crystal, assuming a Lorentzian distribution

$\varrho(\theta)$  is the reliability index of the least-squares fit.

$\sin \theta$	0.05	0.10	0.20	0.30	0.40	0.50	0.60	0.70	0.80	0.90
$A$	0.30	0.30	0.28	0.26	0.22	0.160	0.095	0.030	0.010	-0.16
$B$	0.133	0.133	0.141	0.150	0.146	0.133	0.106	0.051	0.10	0.30
$\varrho$	0.023	0.023	0.023	0.022	0.021	0.020	0.019	0.016	0.020	0.010

( $p_1$  is thus the ordinary polarization factor), the kinematical integrated intensity  $\mathcal{P}_k$  is:

$$\mathcal{P}_k = \mathcal{I}_0 v Q_0 p_1$$

and  $\mathcal{P}$  is given by:

$$\mathcal{P} = \mathcal{P}_k \cdot y$$

with

$$y = (y_{\perp} + y_{\parallel} \cdot \cos^2 2\theta) / (1 + \cos^2 2\theta) \quad (46)$$

or

$$y = (y_{\perp p} \cdot y_{\perp s} + y_{\parallel p} \cdot y_{\parallel s} \cos^2 2\theta) / (1 + \cos^2 2\theta).$$

When a monochromator is used, it follows from Azaroff (1955) that for the perpendicular arrangement of monochromator and specimen diffraction planes, the ordinary polarization factor becomes:

$$p_1' = (\cos^2 2\theta + \cos^2 2\theta_M) / (1 + \cos^2 2\theta_M)$$

(where  $\theta_M$  is the Bragg angle for the monochromator).  $y$  is thus given by:

$$y = (y_{\perp} \cos^2 2\theta_M + y_{\parallel} \cos^2 2\theta) / (\cos^2 2\theta_M + \cos^2 2\theta). \quad (47)$$

A simplified expression for (46) or (47) similar to equation (Z.45) is not recommended, as it is only valid for small values of  $x_0$ .

### III. 2. Absorption effect

Absorption has been neglected in the previous treatment, which is therefore only valid when  $\mu R$  is small. If  $\mu$  is the linear absorption coefficient, equations (10) become:

$$\begin{aligned} \frac{\partial I_0}{\partial x_1} &= -(\bar{\sigma} + \mu)I_0 + \sigma I \\ \frac{\partial I}{\partial x_2} &= -(\bar{\sigma} + \mu)I + \sigma I_0. \end{aligned} \quad (48)$$

The effect of absorption has only to be considered in the real mosaic crystal. The integration of equations (48) is similar to that of equations (10). The result is:

$$\begin{aligned} \varphi(\bar{\sigma}, \mu) &= v^{-1} \mathcal{I}_0^{-1} \int_v dv I_0(x_1, x_2) \exp[-(\mu + \bar{\sigma})T_2'] \quad (49a) \\ &= v^{-1} \int_v dv \mathcal{I}_0(2i\bar{\sigma} / T_1 T_2') \\ &\quad \times \exp[-(\bar{\sigma} + \mu)(T_1 + T_2')]. \end{aligned} \quad (49b)$$

Equation (49b) differs from (17) by a weight  $\exp[-\mu(T_1 + T_2')]$  given to the contribution from each point inside the crystal. The effect of absorption is therefore a lowering of the contribution from the points with a large path length ( $T_1 + T_2'$ ). The importance of this effect can thus be expected to be larger when the Bragg angle increases. Equation (49b) indicates that for the reflections significantly affected by extinction, absorption and extinction are completely correlated. Nevertheless, absorption affects all the reflections and therefore has to be corrected before the structure analysis is started. If  $A(\mu)$  is the absorption

factor, in the absence of extinction, and  $A^*(\mu)$  its inverse, the extinction correction is given by:

$$y_{\mu} = A^*(\mu) v^{-1} \int \varphi(\bar{\sigma}, \mu) \bar{\sigma}(\varepsilon) d\varepsilon_1. \quad (50)$$

One can expand the  $\bar{\sigma}$ -dependent part of the integrand, using (18), which gives with (14):

$$y_{\mu} = \sum_{n=0}^{\infty} (-1)^n \frac{Q^{-1}}{n!} \overline{T_{\mu}^{(n)}} \cdot \int \bar{\sigma}^{n+1} d\varepsilon_1, \quad (51a)$$

where  $\overline{T_{\mu}^{(n)}}$  is given by

$$\overline{T_{\mu}^{(n)}} = A^*(\mu) v^{-1} \int_v T^{(n)} \exp[-\mu(T_1 + T_2')] dv. \quad (51b)$$

Thus,  $\overline{T_{\mu}^{(n)}}$  is the absorption-weighted equivalent of  $T^{(n)}$ .

In particular, if  $\overline{T_{\mu}}$  is the weighted mean path length:

$$\begin{aligned} \overline{T_{\mu}} &= \int_v (T_1 + T_2') \\ &\quad \times \exp[-\mu(T_1 + T_2')] dv / \int_v \exp[-\mu(T_1 + T_2')] dv \\ &= \frac{1}{A^*(\mu)} \cdot \frac{dA^*(\mu)}{d\mu}. \end{aligned} \quad (52)$$

$y_{\mu}$  can be expanded as:

$$y_{\mu} = 1 - \overline{T_{\mu}} Q^{-1} \left\{ \int \bar{\sigma}^2 d\varepsilon_1 \right\} + \dots \quad (53)$$

So, if in the definition of  $X$ ,  $\overline{T}$  is replaced by  $\overline{T_{\mu}}$ , the functional form for the secondary extinction correction remains unchanged in the approximation of equation (37), and  $X$  becomes:

$$X_{\mu} = X \cdot \frac{\overline{T_{\mu}}^{\dagger}}{\overline{T}}. \quad (53b)$$

This first-order approximation:

$$y_{\mu}(X) \simeq y(X_{\mu}) \quad (54)$$

is only valid for small values of  $\theta$  and  $\mu$ . For larger values of  $\mu$  or  $\theta$ ,  $\mu$  must be considered as a new parameter in the evaluation of  $y_{\mu}$ , leading to coefficients  $A(\theta, \mu)$  and  $B(\theta, \mu)$  in (37).

In order to test the range of validity of equation (54) and to get an expression for  $y_{\mu}$  including  $\mu$  as a new parameter, different calculations have been done for a sphere, varying  $\theta$ ,  $X$ , and  $\mu R$ . It follows from the calculations that if  $\overline{T}$  is not replaced by  $\overline{T_{\mu}}$  in the expression for  $X$ , the fit given by (37) cannot be used for  $\mu R \geq 0.25$ . Other expressions for  $\overline{T_{\mu}}$  have been given (Coppens & Hamilton, 1970) as:

$$\overline{T_{\mu}} = -\frac{1}{\mu} \ln A. \quad (55)$$

† The primary extinction parameter  $x$  is unchanged.

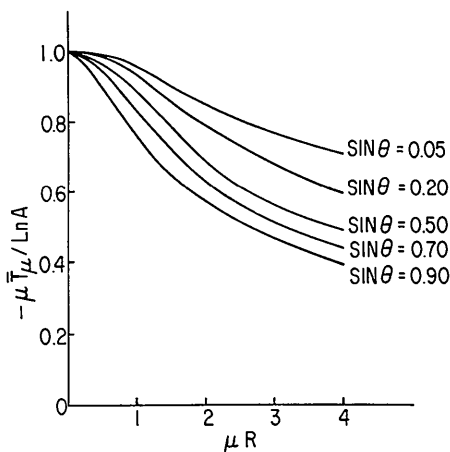


Fig. 8.  $(\bar{T}_\mu/\bar{T}'_\mu)$  versus  $\mu R$  for different Bragg angles  $\theta$ , showing the importance of a correct definition for the absorption-weighted path length  $\bar{T}_\mu$ .

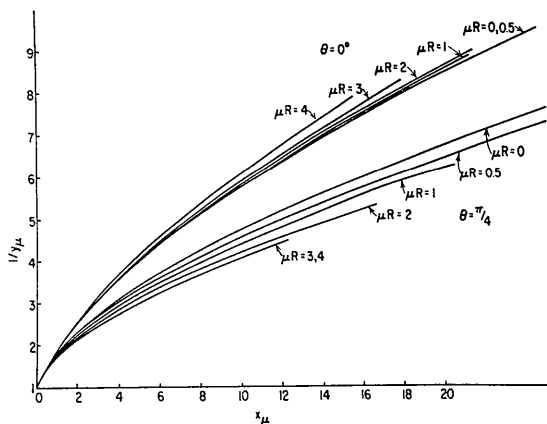


Fig. 9. Influence of the absorption effect on the extinction correction when  $\bar{\sigma}(\epsilon_1)$  is a Lorentzian distribution.

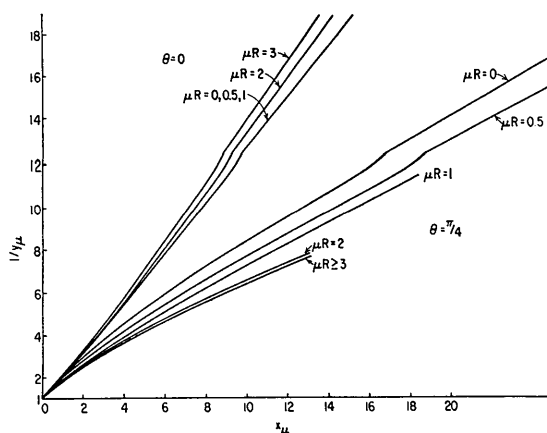


Fig. 10. Influence of the absorption effect on the extinction correction when  $\bar{\sigma}(\epsilon_1)$  is a Gaussian distribution.

Fig. 8 shows that (55) is only equivalent to (52) for small values of  $\mu R$ , and that (52) is the only appropriate form for  $\mu R > 0.25$ . The variation with  $\mu R$  of the curve  $(1/\gamma_\mu)$  as a function of  $X_\mu$ , for different values of  $\theta$ , is shown in Fig. 9 and Fig. 10, for both a Lorentzian distribution and a Gaussian distribution. For small Bragg angles, the approximation (54) is valid when  $\mu R$  is less than unity. But, if  $2\theta$  approaches  $\pi/2$  and  $\mu R > 0.25$ , this approximation cannot be used for large values of  $X_\mu$ . For large Bragg angles, (for which the ratio  $\bar{T}_\mu/\bar{T}$ ) is the smallest),  $X_\mu$  is in general less than 1, so that near  $2\theta = \pi$  (54) is again valid for  $\mu R$  less than 1. The variation of  $\gamma_\mu$  with  $(\mu R)$  for large  $\mu R$  and large angles becomes insignificant.

The least-squares-fitted values for  $A(\theta)$  and  $B(\theta)$  (defined in 37) as a function of  $\mu R$  are given for the two distributions in Tables 7 and 8, for  $\mu R$  smaller than 4.

### Conclusion

It has been shown that the transfer equations (10), even if they only represent incoherently the rescattering processes in a perfect crystal, lead to a reasonable approximate expression for primary extinction in a perfect spherical crystal. Equations (10) are believed to be quite accurate for secondary extinction. An improved expression has been obtained for a spherical crystal, assuming either a Lorentzian or a Gaussian mosaic distribution. The numerical results of the calculation of the extinction correction  $\gamma$  show that the approximation used by Zachariasen (1967) and other authors (Cooper & Rouse, 1970) is only valid when the extinction is very small. The deviation of the actual value of  $\gamma$  from Zachariasen's result is much larger for a Gaussian mosaic distribution than for a Lorentzian distribution especially for Bragg angles not too close to zero. Since Zachariasen's formula for  $\gamma$  has given many satisfactory results (Zachariasen, 1968; Chandreshekar, Ramaseshan & Singh, 1969) it seems likely that the actual distribution is more closely Lorentzian than Gaussian. This conclusion is supported by measurements on large crystals using  $\gamma$ -ray resonance (Maier-Leibnitz, 1972). It has also been shown that the extinction is due to the particle size for small Bragg angles and that if extinction is severe the angular mosaic distribution becomes the dominant effect, while primary extinction can no longer be neglected. The expression for secondary extinction has been modified to allow for absorption effects. In further articles (Becker & Coppens, 1974) results of refinements using these expressions will be considered and the formalism will be extended to crystals of more general shape and to anisotropic extinction.

We gratefully acknowledge partial support of this work by the Petroleum Research Fund administered by the American Chemical Society, and the National Science Foundation.

**APPENDIX A**  
**Integral solution of equations (10)**

From (10b), if one writes:

$$I(x_1, x_2) = a(x_1, x_2) \exp(-\sigma x_2)$$

with the boundary condition:

$$a(x_1, x_2^0) = 0$$

one obtains

$$\partial a / \partial x_2 = \sigma I_0(x_1, x_2) \exp(\sigma x_2).$$

Thus:

$$I(x_1, x_2) = \sigma \exp(-\sigma x_2) \int_{x_2^0}^{x_2} I_0(x_1, u_2) \times \exp(\sigma u_2) du_2. \quad (A1)$$

The total diffracted power  $P(\varepsilon_1)$ , for a given  $\varepsilon_1$ , is:

$$P(\varepsilon_1) = \iint_{\Sigma} I(M_1^2) \mathbf{u}^0 \cdot d\mathbf{s}$$

(Fig. 11). ( $d\mathbf{s} \cdot \mathbf{u}^0$ ) is the surface element  $d\Sigma$  of the orthogonal projection ( $\Sigma$ ) of the crystal, parallel to  $\mathbf{u}^0$ .

$I(x_1, x_2^1)$  at the point  $M_1^2$  is calculated by (A1) and using the expression defining  $P(\varepsilon_1)$ :

$$P(\varepsilon_1) = \iint_{(\Sigma)} d\Sigma \int_{x_2^0}^{x_2^1} \sigma I_0(x_1, x_2) \exp(-\sigma t_2^1) dx_2$$

which may be written as:

$$P(\varepsilon_1) = \int_{\nu} \sigma I_0(x_1, x_2) \exp(-\sigma t_2^1) dv. \quad (A2)$$

In order to calculate (A2),  $I_0(x_1, x_2)$  has to be known. If (10a) is integrated like (10b), one gets (Fig. 2):

$$I_0(x_1, x_2) = \mathcal{J}_0 \exp(-\sigma t_1) + \sigma \exp(-\sigma x_1) \times \int_{x_1^0}^{x_1} I(u_1, x_2) \exp(\sigma u_1) du_1.$$

If  $I(u_1, x_2)$  is calculated by (A1), one gets:

$$I_0(x_1, x_2) = \mathcal{J}_0 \exp(-\sigma t_1) + \sigma^2 \exp[-\sigma(x_1 + x_2)] \times \int_{x_1^0}^{x_1} du_1 \int_{x_2^0}^{x_2} du_2 \{I_0(u_1, u_2) \exp[\sigma(u_1 + u_2)]\}. \quad (A3)$$

**APPENDIX B**  
**Derivation of a general expression for  $\varphi(\sigma)$**

1. The purpose of this Appendix is to show that by an iterative use of the relation (A3) into relation (A2), it is possible to get for  $\varphi(\sigma)$  the solution given in the text by (17). For a given point  $M$  (Fig. 12), the area to be considered in relation (A3) is defined as  $S_1$  (see Fig. 3). For each point  $N_1$  in this domain, the corresponding area  $S_2$  is defined in the same way. For point  $N_k$  in domain  $S_k$ , area  $S_{k+1}$  is defined. The point where the

Table 7. Variation with  $\sin(\theta)$  and  $(\mu R)$  of the coefficients  $A(\theta)$  and  $B(\theta)$  determined by least-squares for a Gaussian distribution

The first number is  $A(\theta)$  and the second  $B(\theta)$ .

$\sin \theta$	0.05	0.10	0.20	0.30	0.40	0.50	0.60	0.70	0.80	0.90
$\mu R$										
	1.28	1.27	1.12	1.02	0.91	0.78	0.65	0.52	0.35	0.20
0.5	-0.008	-0.008	-0.002	0.005	0.010	0.014	0.018	0.028	0.038	0.042
	1.28	1.25	1.05	0.91	0.79	0.68	0.56	0.44	0.30	0.14
1.0	-0.010	-0.010	-0.000	0.011	0.019	0.022	0.026	0.036	0.043	0.035
	1.33	1.30	0.94	0.74	0.61	0.53	0.45	0.34	0.23	0.13
2.0	-0.013	-0.013	0.004	0.027	0.039	0.042	0.039	0.047	0.042	0.019
	1.48	1.43	0.94	0.69	0.56	0.49	0.42	0.33	0.24	0.16
3.0	-0.018	-0.018	0.009	0.044	0.059	0.060	0.050	0.051	0.046	0.030
	1.64	1.59	1.03	0.77	0.64	0.55	0.47	0.35	0.31	0.26
4.0	-0.021	-0.022	0.017	0.066	0.087	0.089	0.071	0.071	0.072	0.090

Table 8. Variation with  $\sin \theta$  and  $(\mu R)$  of the coefficients  $A(\theta)$  and  $B(\theta)$ , determined by least-squares for a Lorentzian distribution

The first number is  $A(\theta)$  and the second is  $B(\theta)$ .

$\sin \theta$	0.05	0.10	0.20	0.30	0.40	0.50	0.60	0.70	0.80	0.90
$\mu R$										
	0.31	0.30	0.26	0.23	0.18	0.12	0.05	0.000	-0.03	-0.30
0.5	0.14	0.14	0.15	0.16	0.16	0.14	0.09		0.05	0.49
	0.32	0.31	0.25	0.19	0.13	0.06	0.000	-0.03	-0.08	-0.35
1.0	0.14	0.14	0.16	0.18	0.18	0.13		0.05	0.08	0.50
	0.37	0.35	0.21	0.13	0.00	0.00	-0.10	-0.20	-0.37	-0.53
2.0	0.17	0.16	0.18	0.40			0.30	0.48	0.63	0.69
	0.45	0.44	0.24	0.03	0.00	-0.06	-0.11	-0.20	-0.35	-0.44
3.0	0.20	0.20	0.25	0.09		0.14	0.29	0.49	0.57	0.60
	0.58	0.56	0.32	0.07	0.00	-0.02	-0.04	-0.18	-0.21	-0.26
4.0	0.24	0.24	0.37	0.40		-0.03	-0.02	0.29	0.29	0.31

incident beam through  $N_k$  intersects the diffracted beam through  $M$  is defined as  $M_k$ . Using relation (A3) iteratively,  $\varphi(\sigma)$  can be written [from equation (15) of the text] as:

$$\begin{aligned} \varphi(\sigma) &= v^{-1} \sum_{k=0}^{\infty} \sigma^{2k} \int_v dv(M) \int_{S_1} d\Sigma(N_1) \\ &\times \int_{S_2} d\Sigma(N_2) \int_{S_k} d\Sigma(N_k) \\ &\times \exp \{ -\sigma[t_1(M_k) + t'_2(M_k)] \} \end{aligned} \quad (B1)$$

where  $d\Sigma(N_k) = du_1(N_k) du_2(N_k)$ .

The first term in the summation (B1) is given by

$$\varphi_0(\sigma) = v^{-1} \int_v dv \exp [ -\sigma(t_1 + t'_2) ] \quad (B2)$$

and corresponds to the first-order approximation.

The second term  $\varphi_1(\sigma)$ , allowing for twofold ex-

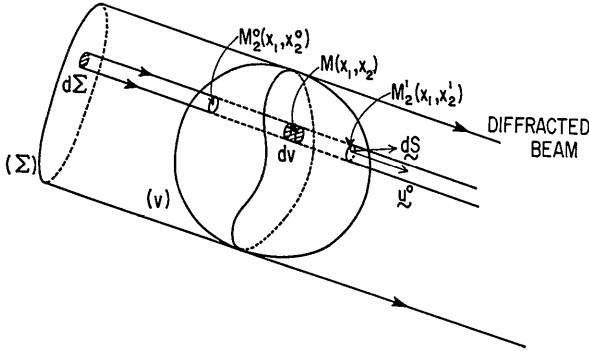


Fig. 11. Projection ( $\Sigma$ ) of a crystal of general shape on the plane perpendicular to the diffracted beam  $u^0$ .

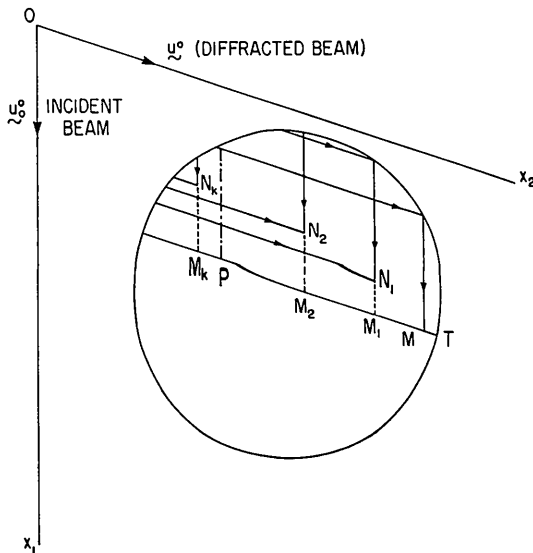


Fig. 12. Definition of the nest of domains ( $S_i$ ) corresponding to the points  $N_i$ , such that  $N_{i+1}$  is always preceding  $N_i$ .

change of radiation between  $I_0$ ,  $I$  and feedback to  $I_0$ , is given by:

$$\begin{aligned} \varphi_1(\sigma) &= v^{-1} \sigma^2 \int_v dv(M) \int_{S_1} d\Sigma(N_1) \\ &\times \exp \{ -\sigma[t_1(M_1) + t'_2(M_1)] \}. \end{aligned}$$

The integrand is independent of the coordinate  $u_1$  of  $N_1$  and it is possible to first integrate over  $u_1$ :

$$\begin{aligned} \varphi_1(\sigma) &= v^{-1} \sigma^2 \int_v dv(M) \int_{u_2^0}^{u_2(M)} du_2(M_1) \\ &\times \min \{ t_1(M), t_1(M_1) \} \exp \{ -\sigma[t_1(M_1) + t'_2(M_1)] \} \end{aligned}$$

where  $\min \{ t_1(M), t_1(M_1) \}$  is the smallest of these two path lengths. At this point, it is necessary to introduce an approximation:  $\min \{ t_1(M), t_1(M_1) \}$  will be replaced by  $t_1(M_1)$ . It is only an approximation when  $M$  belongs to the domain ( $B$ ) of Fig. 3 and if point  $M_1$ , is between  $M$  and  $P$  (Fig. 12). For small Bragg angles, the error introduced by this approximation is very small. For high Bragg angles, the effect of this approximation will be to overestimate  $\varphi(\sigma)$ , which will be closer to 1. The next step is to interchange the integrations over points  $M_1$  and  $M$ :

$$\begin{aligned} \varphi_1(\sigma) &= v^{-1} \sigma^2 \int_v dv(M_1) \exp \{ -\sigma[t_1(M_1) + t'_2(M_1)] \} \\ &\times t_1(M_1) \int_{M_1}^T du_2(M) \end{aligned}$$

[since  $dv(M) \cdot du_2(M_1) = dv(M_1) \cdot du_2(M)$ ]

$$\varphi_1(\sigma) = v^{-1} \sigma^2 \int_v dv t_1 t'_2 \exp [ -\sigma(t_1 + t'_2) ]. \quad (B3)$$

Analogously, it is possible to show that:

$$\varphi_k(\sigma) = v^{-1} \sigma^{2k} \int_v dv \frac{(t_1 t'_2)^k}{(k!)^2} \exp [ -\sigma(t_1 + t'_2) ]. \quad (B4)$$

$\varphi(\sigma)$  is thus given by:

$$\varphi(\sigma) = \sum_{k=0}^{\infty} \varphi_k(\sigma).$$

$$\varphi(\sigma) = v^{-1} \int_v dv \exp [ -\sigma(t_1 + t'_2) ] \cdot \sum_{k=0}^{\infty} \frac{(\sigma^2 t_1 t'_2)^k}{(k!)^2}. \quad (B5)$$

It can be shown (Abramowitz & Segun, 1965) that:

$$\varphi(\sigma) = v^{-1} \int_v dv \exp [ -\sigma(t_1 + t'_2) ] \mathcal{S}_0[2i\sigma\sqrt{t_1 t'_2}], \quad (B6)$$

where  $\mathcal{S}_0(x)$  is a zero-order Bessel function.

2. It will be shown that equation (B5) can be written as a power series similar to equation (Z.14) with  $t_2$  and  $t'_2$  interchanged. If the exponential term is written as a series expansion, the integrand of (B5):

$$\varrho = \exp [ -(\xi + \eta) ] \sum_{k=0}^{\infty} \frac{(\xi \eta)^k}{(k!)^2}$$

where  $(\xi = \sigma t_1, \eta = \sigma t_2')$  becomes:

$$\varrho = \sum_{k=0}^{\infty} \sum_{n=0}^{\infty} (-1)^n \frac{(\xi\eta)^k [\xi + \eta]^n}{n!(k!)^2}.$$

$\varrho$  can be written as:

$$\varrho = \sum_{t=0}^{\infty} (-1)^t \frac{A_t}{t!}$$

where the power of  $A_t$  with respect to both variables  $\xi$  and  $\eta$  is  $t$ . The calculation of  $A_t$  for  $t$  even will be developed ( $t=2s$ ):

$$A_{2s} = \sum_{p=0}^s \sum_{j=0}^{2p} \xi^{s-p+j} \eta^{s+p-j} \frac{2s!}{[(s-p)!j!(2p-j)!]}.$$

If  $r$  is defined as:

$$r = s - p + j$$

it is clear that

$$s + p - j = 2s - r.$$

$A_{2s}$  may be written as:

$$A_{2s} = \sum_{r=0}^{2s} \xi^r \eta^{2s-r} \chi_r$$

with

$$\begin{aligned} \chi_r &= \sum_{j=0}^n \frac{2s!}{[(r-j)!]^2 (2s-2r+j)! j!} \\ &= \binom{2s}{r} \sum_{j=0}^r \binom{r}{r-j} \binom{2s-r}{j} \end{aligned}$$

$$\chi_r = \binom{2s}{r}^2 \quad (\text{Abramowitz \& Segun, 1965}).$$

The final result is:

$$A_{2s} = \sum_{r=0}^{2s} \xi^r \eta^{2s-r} \binom{2s}{r}^2.$$

Using similar arguments for odd values of  $t$ , it is easy to show that:

$$\varphi(\sigma) = \sum_{n=0}^{\infty} (-1)^n \frac{\sigma^n}{n!} \overline{t^{(n)}}. \quad (B7)$$

With

$$\overline{t^{(n)}} = v^{-1} \int_v^n dv \sum_{j=0}^n \binom{n}{j}^2 t_1^j t_2'^{n-j}$$

(B7) is similar to (Z. 14) with  $t_2$  and  $t_2'$  interchanged.

3. This Appendix will be concluded by studying the limiting cases ( $2\theta=0$ ) and  $2\theta=\pi$ . For ( $2\theta=0$ ), the solution of equation (10) becomes a one-dimensional problem ( $t_1=t_2=t$ ;  $t_2'=l-t$ ) (Fig. 13). One gets easily

$$\varphi^0(\sigma) = v^{-1} \int_v^l dv \exp[-2\sigma t]. \quad (B8)$$

It will be shown that in this limit the approximation (B5) gives the same value as (B8). From (B5):

$$\varphi(\sigma) = v^{-1} \int_v^l \exp(-\sigma l) \sum_{k=0}^{\infty} \frac{\sigma^{2k}}{(k!)^2} t^k (l-t)^k dv.$$

If one defines the surface element  $d\Sigma$  (Fig. 13) by

$$dv = d\Sigma dt,$$

it follows that:

$$\varphi(\sigma) = v^{-1} \iint_{\Sigma} d\Sigma \exp(-\sigma l) \int_0^l \sum_{k=0}^{\infty} \frac{\sigma^{2k}}{(k!)^2} t^k (l-t)^k dt.$$

Since:

$$\sigma^{2n} \int_0^l \frac{t^n (l-t)^n}{(n!)^2} dt = \sigma^{2n} \frac{l^{2n+1}}{(2n+1)!}$$

one gets

$$\varphi(\sigma) = v^{-1} \iint_{\Sigma} \frac{\sinh(\sigma l)}{\sigma} \exp(-\sigma l) d\Sigma. \quad (B9a)$$

Integration of (B8) along the incident direction gives:

$$\varphi^0(\sigma) = v^{-1} \iint_{\Sigma} d\Sigma \int_0^l \exp(-2\sigma t) dt. \quad (B9b)$$

Since expressions (B9a) and (B9b) are equal:

$$\varphi^0(\sigma) = \varphi(\sigma).$$

For  $2\theta=\pi$ , the integration of equations (10) gives the result:

$$\varphi^{\pi}(\sigma) = v^{-1} \int_v^l \frac{dv}{1+\sigma l} \quad (B10)$$

which differs from the approximate value given by (B7).

### APPENDIX C

#### Derivation of $\sigma(\epsilon_1)$ for a convex crystal

From equation (2)

$$I_k(\epsilon) = \mathcal{F}_0 \left| \frac{aFK}{R_0} \right|^2 \left| \sum_{\mathbf{L}} \exp[2\pi i \epsilon \cdot \mathbf{L}/\lambda] \right|^2.$$

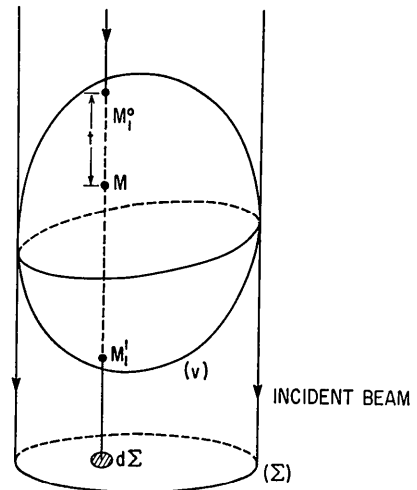


Fig. 13. Geometry for  $2\theta=0$  and  $2\theta=\pi$ ;  $l = M_1^0 M_1^l$ . (a)  $2\theta=0$ ,  $t_1=t$ ,  $t_2=l-t$ . (b)  $2\theta=\pi$ ,  $t_1=t_2=t$ .

From (3) and (4):

$$\sigma(\varepsilon_1) = Q \frac{V^2}{v} \frac{\sin 2\theta}{\lambda^3} A, \quad (C1)$$

where  $A$  is defined by:

$$A = \iint d\varepsilon_2 d\varepsilon_3 \left| \sum_{\mathbf{L}} \exp(2\pi i \varepsilon \cdot \mathbf{L}/\lambda) \right|^2. \quad (C2)$$

If in (C2) the summation over the lattice points is replaced by an integral over the volume of the crystal:

$$\sum_{\mathbf{L}} \exp(2\pi i \varepsilon \cdot \mathbf{L}/\lambda) \simeq V^{-1} \int_v \exp(2\pi i \varepsilon \cdot \mathbf{r}/\lambda) dv, \quad (C3)$$

$A$  becomes:

$$A = \int_v dv \int_v dv' \int_{-\infty}^{+\infty} d\varepsilon_2 \int_{-\infty}^{+\infty} d\varepsilon_3 \times \exp[2\pi i \varepsilon \cdot (\mathbf{r} - \mathbf{r}')/\lambda]. \quad (C4)$$

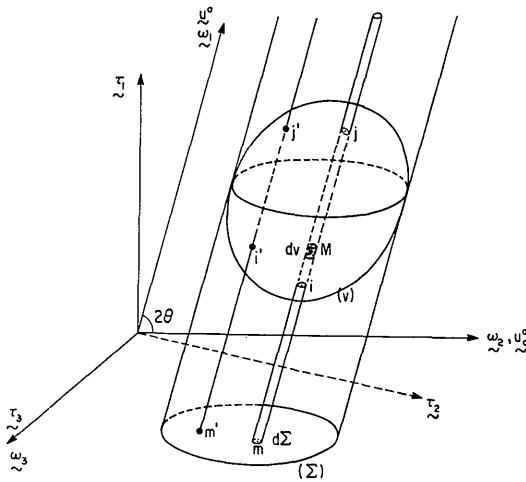


Fig. 14. Projection of the crystal parallel to the diffracted beam, onto the plane defined by the incident beam and the normal to the diffraction plane.  $m$  is a point of the projection ( $\Sigma$ ).  $i$  and  $j$  are the point of entrance and the point of exit of the parallel to  $\mathbf{u}^0$  through  $M$ .  $l$  is equal to  $\bar{i}\bar{j}$ .

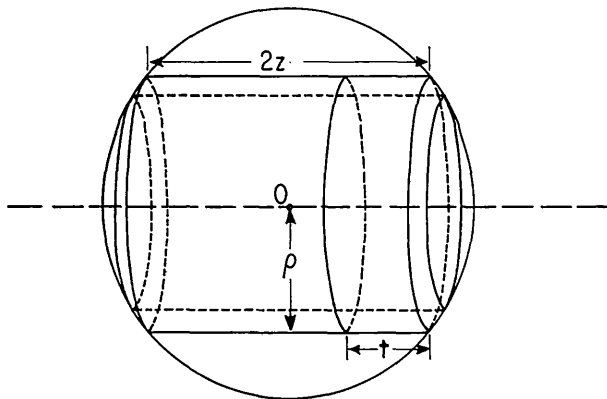


Fig. 15. The cylindrical coordinate system ( $z, \rho$ ).  $z$  and  $\rho$  are related by:  $\rho^2 + z^2 = r^2$ .

Reciprocal space is referred to axes  $\{\tau_1, \tau_2, \tau_3\}$ , defined in Fig. 14. If direct space is referred to the reciprocal of the previous frame, its unit axis are  $\omega_1$ , parallel to  $\mathbf{u}^0$ ,  $\omega_2$  parallel to  $\mathbf{u}_2^0$ ,  $\omega_3$  parallel to  $\tau_3$  (Fig. 14). Thus (C4) transforms to:

$$\begin{aligned} A &= \int_v \int_v dv dv' \exp[2\pi i \varepsilon_1 (r_1 - r'_1) \sin 2\theta/\lambda] \\ &\times \int_{-\infty}^{+\infty} \exp[2\pi i \varepsilon_2 (r_2 - r'_2) \sin 2\theta/\lambda] d\varepsilon_2 \\ &\times \int_{-\infty}^{+\infty} \exp[2\pi i \varepsilon_3 (r_3 - r'_3)/\lambda] d\varepsilon_3 \\ &= \int_v \int_v dv dv' \exp[2\pi i \varepsilon_1 (r_1 - r'_1) \sin 2\theta/\lambda] \\ &\times \delta[(r_2 - r'_2) \sin 2\theta/\lambda] \delta[(r_3 - r'_3)/\lambda]. \end{aligned}$$

Because, for a Dirac distribution,

$$\delta(kx) = |k|^{-1} \delta(x),$$

$A$  can be written as:

$$A = \frac{\lambda^2}{\sin 2\theta} \int_v \int_v dv dv' \exp[2\pi i \varepsilon_1 (r_1 - r'_1) \sin 2\theta/\lambda] \times \delta(r_2 - r'_2) \delta(r_3 - r'_3). \quad (C5)$$

Since for a convex crystal

$$dv = dr_1 dr_2 dr_3 \sin 2\theta = d\Sigma d(\overline{mM}) \cdot \sin 2\theta,$$

(C5) can be written as:

$$\begin{aligned} A &= \lambda^2 \sin 2\theta \int_{\Sigma} \int_{\Sigma'} d\Sigma d\Sigma' \delta(m - m') \\ &\times \int_i^j \exp[2\pi i \varepsilon_1 \overline{mM} \sin 2\theta/\lambda] d(\overline{mM}) \\ &\times \int_{i'}^{j'} \exp[-2\pi i \varepsilon_1 \overline{m'M'} \sin 2\theta/\lambda] d(\overline{m'M'}). \end{aligned}$$

$\overline{mi}$  and  $\overline{mj}$  are functions of  $m$  only. If  $f(m)$  is defined as:

$$f(m) = \int_i^j \exp[2\pi i \varepsilon_1 \overline{mM} \sin 2\theta/\lambda] d(\overline{mM}),$$

$A$  becomes:

$$\begin{aligned} A &= \lambda^2 \sin 2\theta \int_{\Sigma} d\Sigma f(m) \int_{\Sigma'} f^*(m') \delta(m - m') d\Sigma' \\ A &= \lambda^2 \sin 2\theta \int_{\Sigma} d\Sigma |f(m)|^2. \end{aligned} \quad (C6)$$

$\bar{i}\bar{j}$ , which is the thickness of the crystal parallel to the diffracted beam, is written as  $l(m)$ . Thus:

$$|f(m)|^2 = l^2 \frac{\sin^2 [\pi \varepsilon_1 l \sin 2\theta/\lambda]}{[\pi \varepsilon_1 l \sin 2\theta/\lambda]^2}.$$

If the quantity  $\alpha$  is defined as:

$$\alpha = l \sin 2\theta/\lambda$$

$$|f(m)|^2 = l^2 \frac{\sin^2 (\pi \varepsilon_1 \alpha)}{(\pi \varepsilon_1 \alpha)^2}.$$



If  $dv$  is written as:

$$dv = d\Sigma \cdot l \sin 2\theta$$

the final result becomes:

$$\sigma(\varepsilon_1) = Qv^{-1} \int_v dv \alpha \frac{\sin^2(\pi\varepsilon_1\alpha)}{(\pi\varepsilon_1\alpha)^2}. \quad (C7)$$

**APPENDIX D**

**Some mathematical derivations for spherical crystals**

*Derivation of  $\sigma(\varepsilon_1)$*

With the notations of Fig. 15, and choosing the  $x$  axis to be parallel to the diffracted beam  $u^0$ , one gets, as the integrand in equation (19a) is only dependent on  $z$  ( $l=2z$ ),

$$dv = 4\pi z^2 dz$$

$$\sigma(\varepsilon_1) = v^{-1} Q \int_0^r 4\pi z^2 dz \frac{\sin^2(2\pi z \varepsilon_1 \sin 2\theta/\lambda)}{(2\pi z \varepsilon_1 \sin 2\theta/\lambda)^2} \cdot 2z \sin 2\theta/\lambda$$

which, by integration gives (29).

*Mean values of simple functions of the path lengths in spheres*

The mean over the volume of the  $n$ th power of the thickness  $l$  of the crystal can be evaluated as follows:

$$\bar{l}^n = v^{-1} \int_v dv \cdot l^n = v^{-1} \int_0^r 4\pi z^2 dz \cdot (2z)^n$$

$$\bar{l}^n = \frac{2^n \cdot 3(r)^n}{n+3}. \quad (D1)$$

The mean over the volume of the  $n$ th power of the depth  $t_1$  or  $t_2$  parallel to the incident or the diffracted beam is given by (with the notations of Fig. 15):

$$\bar{t}_1^n = \bar{t}_2^n = \bar{t}^n = v^{-1} \int_0^r 2\pi \rho d\rho \int_0^{2z} t^n dt$$

$$= v^{-1} \int_0^r 4\pi \rho z d\rho \frac{2^n z^n}{n+1}.$$

Since  $\rho d\rho + z dz = 0$ , one gets

$$\bar{t}^n = \frac{2^n \cdot 3 \cdot (r)^n}{(n+1)(n+3)}. \quad (D2) \text{ (Z.17)}$$

For  $2\theta=0$ :

$$\bar{t}^{(n)}(0) = 2^n \bar{t}^n \quad (D3a)$$

where  $\bar{t}^{(n)}$  is defined in (18b).

For  $2\theta=\pi$  since

$$t_1 = t_2 = t$$

one gets

$$\bar{t}^{(n)}(\pi) = \bar{t}^n \cdot \sum_j \binom{n}{j}^2 = \bar{t}^n \sum_j \binom{n}{j} \binom{n}{n-j} = \bar{t}^n \binom{2n}{n}. \quad (D3b)$$

*Calculation of diffracting cross sections in real crystals*

$\bar{\sigma}(\varepsilon_1)$ , defined by (21):

$$\bar{\sigma}(\varepsilon_1) = \sigma * W$$

will be calculated for a Gaussian or a Lorentzian mosaic distribution:

$$W_G = \sqrt{2g} \exp(-2\pi\varepsilon^2 g^2)$$

$$W_L = 2g/(1+4\pi^2\varepsilon^2 g^2).$$

If  $F$  and  $F^{-1}$  are the Fourier transform and inverse Fourier transform operators,

$$\sigma * W = F^{-1}(F\sigma F W) \equiv F^{-1}(\chi \cdot \omega).$$

The Fourier transform  $\chi(\eta)$  of  $W$  is given by:

$$\chi_G = \exp[-\pi\eta^2/2g^2]$$

$$\chi_L = \exp(-|\eta|/g).$$

The Fourier transform of the integrand of (19a)

$$d(\varepsilon) = \alpha \frac{\sin^2(\pi\varepsilon\alpha)}{(\pi\varepsilon\alpha)^2}$$

is given by

$$\omega(\eta) = (1 - |\eta|/\alpha) \text{ if } |\eta| < \alpha$$

$$= 0 \text{ otherwise.}$$

Because  $\alpha = 2z \sin 2\theta/\lambda$ , with the notation of Fig. 15, one gets by inverse Fourier transform of  $(\chi \cdot \omega)$ :

*Lorentzian distribution*

$$\bar{\sigma}_L(\varepsilon_1) = \frac{3Q}{\beta^3} \int_0^\beta \alpha^2 d\alpha \int_0^\alpha 2 \left(1 - \frac{x}{\alpha}\right) \times \exp(-x/g) \cos 2\pi\varepsilon_1 x dx \quad (D4)$$

which can be analytically integrated. The result is a complicated function of both parameters  $\beta$  and  $g$ .

*Gaussian distribution*

$$\bar{\sigma}_G(\varepsilon_1) = \frac{3Q}{\beta^3} \int_0^\beta \alpha^2 d\alpha \int_0^\alpha 2 \left(1 - \frac{x}{\alpha}\right) \times \exp(-\pi x^2/2g^2) \cos 2\pi\varepsilon_1 x dx \quad (D5)$$

which can only be integrated using transcendental functions.

The solutions given by (D4) and (D5) are not suited for an easy use in integration of  $\{\bar{\sigma}\varphi(\bar{\sigma})\}$ .

However, if  $\sigma(\varepsilon)$  is approximated either by a Lorentzian or a Gaussian distribution, the derivation of  $\bar{\sigma}(\varepsilon)$  becomes straightforward. The approximations for  $\sigma(\varepsilon)$  are given by:

$$\sigma_G(\varepsilon_1) = Q\bar{\alpha} \exp(-\pi\varepsilon_1^2 \bar{\alpha}^2) \quad (Z.35)$$

$$\sigma_L(\varepsilon_1) = Q\frac{4}{3}\bar{\alpha}/[1+(\frac{4}{3}\pi\varepsilon_1\bar{\alpha})^2]. \quad (Z.26)$$

Writing  $\bar{\sigma}(\varepsilon)$  respectively as:

$$\bar{\sigma}_L(\varepsilon_1) = \sigma_L(\varepsilon_1) * W_L(\varepsilon_1) \quad (D6a)$$

$$\bar{\sigma}_G(\varepsilon_1) = \sigma_G(\varepsilon_1) * W_G(\varepsilon_1), \quad (D6b)$$

one obtains:

$$\bar{\sigma}_L(\varepsilon_1) = \frac{4}{3}Q\alpha_L/[1+\frac{4}{3}\pi\varepsilon_1\alpha_L]^2 \quad (D7)$$

with	$\alpha_L = \bar{\alpha} / \left(1 + \frac{2\bar{\alpha}}{3g}\right)$	$Q$	Average scattering cross section per unit volume of crystal, $\text{cm}^{-1}$ .
and	$\bar{\sigma}_G(\varepsilon_1) = Q\alpha_G \exp(-\pi\varepsilon_1^2\alpha_G^2)$ (D8)	$Q_0$	Same as $Q$ for $K=1$ .
with	$\alpha_G = \bar{\alpha} / \left(1 + \frac{\bar{\alpha}^2}{2g^2}\right)^{1/2}$	$r$	Radius of an ideal spherical crystal.
		$R$	Radius of a mosaic spherical crystal.
		$R_0$	The distance between the crystal and the counter.
		$S$	Diffraction vector: $(\mathbf{u} - \mathbf{u}_0)/\lambda$ .
		$t_1$	Depth along the incident direction.
		$t_2$	Depth along the diffracted direction.
		$t_2'$	Distance along the diffracted beam between a point and the exit from the crystal.
		$T_1, T_2'$	Same path lengths as $t_1$ and $t_2'$ , for a mosaic crystal.
		$t$	Mean path length through a perfect crystal ( $\frac{2}{3}r$ for a sphere).
		$\overline{t^{(n)}}$	Mean value over the crystal volume of $\sum_j \binom{n}{j} t_1^j t_2^{n-j}$ .
		$\overline{T^{(n)}}$	Same as $\overline{t^{(n)}}$ , for a mosaic crystal.
		$\bar{T}$	Mean path length through a mosaic crystal ( $\frac{2}{3}R$ for a sphere).
		$\overline{T_\mu}$	The absorption-weighted mean path length through the real crystal.
		$\overline{t_\mu^{(n)}}$	The equivalent of $\overline{t^{(n)}}$ when absorption is not negligible.
		$\mathbf{u}_0, \mathbf{u}$	Unit vectors parallel to the directions of the incident and diffracted beams.
		$\mathbf{u}_0^0, \mathbf{u}^0$	Particular values of $\mathbf{u}_0$ and $\mathbf{u}$ when Bragg condition is exactly fulfilled.
		$v$	Volume of the crystal, $\text{cm}^3$ .
		$V$	Volume of the unit cell, $\text{\AA}^3$ .
		$W(\eta)$	Angular distribution of the crystallite inside a real crystal.
		$x_1, x_2, x_3$	Coordinates of a point inside the crystal, along axes parallel to the incident direction, the diffracted direction and the perpendicular to the diffraction plane.
		$x$	The extinction parameter: $\frac{2}{3}Q\bar{\alpha}t$ for a perfect crystal.
		$x_0$	The value of $x$ for $K=1$ .
		$X$	The extinction parameter: $\frac{2}{3}Q\alpha_{G,L}\bar{T}$ for a mosaic crystal.
		$X_0$	The value of $X$ for $K=1$ .
		$X_\mu$	The extinction parameter when absorption is present $X_\mu = X\bar{T}_\mu/\bar{T}$ .
		$y$	The extinction correction: $\mathcal{P}/\mathcal{P}_k$
		$y_p, y_s$	Primary and secondary extinction corrections.
		$y_{\parallel}, y_{\perp}$	Extinction corrections for the parallel or perpendicular component of the X-ray electric field.
		$y_\mu$	The extinction correction when absorption is not negligible.
		$\alpha$	Parameter: $\frac{l \sin 2\theta}{\lambda}$
		$\bar{\alpha}$	The mean value of $\alpha$ over the crystal volume ( $\frac{2}{3}r \sin 2\theta/\lambda$ for a sphere of radius $r$ ).

## APPENDIX E

## Glossary of symbols

$a$	$10^{-12}$ cm for neutron diffraction $\left(\frac{e^2}{mc^2}\right)$ for X-ray diffraction.
$A(\mu)$	The transmission factor.
$A^*(\mu)$	The quantity $[1/A(\mu)]$ .
$A(\theta), B(\theta)$	Least-squares fitted coefficients occurring in the expression for $y$ .
$F$	The structure factor in cm (unit cell) $^{-1}$ for neutrons, in electrons (unit cell) $^{-1}$ for X-rays.
$g$	Width parameter of the mosaic distribution.
$H$	A reciprocal vector: particular value of $S$ when the Bragg condition is fulfilled.
$I_0(M)$	Intensity of the incident beam in direction $\mathbf{u}_0$ , at a point $M$ inside the crystal, $\text{cm}^{-2} \text{sec}^{-1}$ .
$I(M)$	The intensity of the scattered radiation in direction $\mathbf{u}$ , at point $M$ inside the crystal, $\text{cm}^{-2} \text{sec}^{-1}$ .
$I_k(\varepsilon)$	The intensity of radiation scattered in direction $\mathbf{u}$ , in the kinematical approach, $\text{cm}^{-2} \text{sec}^{-1}$ .
$\mathcal{I}_0$	The intensity of the incident beam before it strikes the crystal, $\text{cm}^{-2} \text{sec}^{-1}$ .
$K$	The coefficient of polarization: 1 for neutron diffraction; 1 for the parallel component of X-ray electric field; $\cos 2\theta$ for the perpendicular component of X-ray electric field.
$l$	Local thickness of the crystal parallel to the diffracted beam.
$\mathbf{L}$	A lattice vector in the crystal.
$P_k(\varepsilon_1)$	The power recorded in the counter for a given direction of the incident beam, in the kinematical approach, $\text{sec}^{-1}$ .
$P(\varepsilon_1)$	The power recorded in the counter, for a real crystal, $\text{sec}^{-1}$ .
$\mathcal{P}_k$	Integrated intensity of a Bragg reflection in the kinematical approximation, $\text{sec}^{-1}$ .
$\mathcal{P}$	Integrated intensity of a Bragg reflection in a real crystal, $\text{sec}^{-1}$ .
$\mathcal{P}_{\parallel}, \mathcal{P}_{\perp}$	Values of $\mathcal{P}$ for the parallel and perpendicular components of the X-ray electric field.

$\alpha_G, \alpha_L$  Quantities analogous to  $\alpha$ , for a mosaic crystal, corresponding to a Gaussian or to a Lorentzian mosaic distribution.

$\beta$  The quantity  $\frac{4}{3}\alpha$ .

$\varepsilon$  (S-H). The component of  $\varepsilon$  along the vector  $\tau_i$  is the small angle  $\varepsilon_i$  ( $i=1,2,3$ ).  $\varepsilon_1$ : divergence of the incident beam.

$\theta$  Bragg angle.

$\theta_M$  Bragg angle of the monochromator.

$\lambda$  Wavelength of the radiation, Å.

$\mu$  The linear absorption coefficient,  $\text{cm}^{-1}$ .

$\sigma(\varepsilon_1)$  Diffracting cross section per unit of volume and intensity,  $\text{cm}^{-1}$ .

$\bar{\sigma}(\varepsilon_1)$  Average diffracting unit cross section in a mosaic crystal.

$\tau_1$  Unit vector in the diffraction plane, perpendicular to  $\mathbf{u}_0^0$ .

$\tau_2$  Unit vector in the diffraction plane, perpendicular to  $\mathbf{u}^0$ .

$\tau_3$  Unit vector along the vertical axis, (perpendicular to the diffraction plane).

$\varphi(\sigma)$  Extinction correction function for a given direction of the incident beam.

$\varphi^0(\sigma), \varphi^\pi(\sigma)$  Exact solutions for  $\varphi(\sigma)$  for  $2\theta=0$  and  $2\theta=\pi$ .

## References

- ABRAMOWITZ, M. & SEGUN, I. A. (1965). *Handbook of Mathematical Functions*. New York: Dover Press.
- AUTHIER, A. (1970). *Advances in Structure Research by Diffraction Methods* (3), pp. 1–52. Oxford: Pergamon Press.
- AZAROFF, L. V. (1955). *Acta Cryst.* **8**, 701–704.
- AZAROFF, L. V. (1964). *Advanced Methods in X-ray Crystallography*. Edited by G. N. RAMACHANDRAN. pp. 251–269. New York: Academic Press.
- AZAROFF, L. V. (1968). *Elements of X-ray Crystallography*. pp. 186–228. New York: McGraw-Hill.
- BECKER, P. J. & COPPENS, P. (1974). *Acta Cryst.* **A30**, 148–153, and to be published.
- CHANDRASEKHAR, S. (1956). *Acta Cryst.* **9**, 954–956.
- CHANDRASEKHAR, S., RAMASESHAN, S. & SINGH, A. K. (1969). *Acta Cryst.* **A25**, 140–142.
- COOPER, M. J. (1970). *Acta Cryst.* **A26**, 208–213.
- COOPER, M. J. & ROUSE, K. D. (1970). *Acta Cryst.* **A26**, 213–223.
- COOPER, M. J. & ROUSE, K. D. (1971). *Acta Cryst.* **A27**, 622–628.
- COPPENS, P. (1969). *Crystallographic Computing*. Edited by F. R. AHMED, pp. 255–270. Copenhagen: Munksgaard.
- COPPENS, P. & HAMILTON, W. C. (1970). *Acta Cryst.* **A26**, 71–83.
- EKSTEIN, H. (1951). *Phys. Rev.* **83**, 721–729.
- HAMILTON, W. C. (1957). *Acta Cryst.* **10**, 629–634.
- HAMILTON, W. C. (1963). *Acta Cryst.* **16**, 609–611.
- JAMES, R. W. (1957). *The Optical Principles of the Diffraction of X-rays*. pp. 34–66, 268–336. London: Bell.
- JAMES, R. W. (1963). *The Dynamical Theory of X-ray Diffraction, Solid State Physics*. Vol. 15, pp. 53–220. New York: Academic Press.
- LARSON, A. C. (1969). *Crystallographic Computing*. Edited by F. R. AHMED. pp. 291–294. Copenhagen: Munksgaard.
- LAWRENCE, J. L. (1972). *Acta Cryst.* **A28**, 400–404.
- MAIER-LEIBNITZ, H. (1972). Proceedings of the Advanced Institute on the Experimental Aspects of X-ray and Neutron Diffraction, Aarhus–Denmark.
- SEQUEIRA, A., RAJAGOPAL, H. & CHIDAMBARAM, R. (1972a). *Acta Cryst.* **B28**, 2514–2519.
- SEQUEIRA, A., RAJAGOPAL, H. & CHIDAMBARAM, R. (1972b). *Acta Cryst.* **A28**, S4, S193.
- TAKAGI, S. (1961). *Acta Cryst.* **15**, 1311–1312.
- WEISS, R. G. (1952). *Proc. Phys. Soc.* **B65**, 553–555.
- WERNER, A. S. (1969). *Acta Cryst.* **A25**, 639.
- ZACHARIASEN, W. H. (1945). *Theory of X-ray Diffraction in Crystals*. pp. 89–176. New York: John Wiley.
- ZACHARIASEN, W. H. (1963). *Acta Cryst.* **16**, 1139–1144.
- ZACHARIASEN, W. H. (1965). *Trans. Amer. Cryst. Assoc.* **1**, 33–41.
- ZACHARIASEN, W. H. (1967). *Acta Cryst.* **23**, 558–564.
- ZACHARIASEN, W. H. (1968a). *Acta Cryst.* **A24**, 212–216.
- ZACHARIASEN, W. H. (1968b). *Acta Cryst.* **A24**, 324–325.
- ZACHARIASEN, W. H. (1968c). *Acta Cryst.* **A24**, 425–427.
- ZACHARIASEN, W. H. (1968d). *Acta Cryst.* **A24**, 421–424.
- ZACHARIASEN, W. H. (1969). *Acta Cryst.* **A25**, 102.